

DC-LA: Difference-of-Convex Langevin Algorithm

Hoang Phuc Hau Luu* Zhongjian Wang†

February 2, 2026

Abstract

We study a sampling problem whose target distribution is $\pi \propto \exp(-f - r)$ where the data fidelity term f is Lipschitz smooth while the regularizer term $r = r_1 - r_2$ is a non-smooth difference-of-convex (DC) function, i.e., r_1, r_2 are convex. By leveraging the DC structure of r , we can smooth out r by applying Moreau envelopes to r_1 and r_2 separately. In line of DC programming, we then redistribute the concave part of the regularizer to the data fidelity and study its corresponding proximal Langevin algorithm (termed DC-LA). We establish convergence of DC-LA to the target distribution π , up to discretization and smoothing errors, in the q -Wasserstein distance for all $q \in \mathbb{N}^*$, under the assumption that V is distant dissipative. Our results improve previous work on non-log-concave sampling in terms of a more general framework and assumptions. Numerical experiments show that DC-LA produces accurate distributions in synthetic settings and reliably provides uncertainty quantification in a real-world Computed Tomography application.

1 Introduction

The sampling problem from a Gibbs distribution in \mathbb{R}^d under the form $\pi \propto e^{-V}$ is fundamental in machine learning and Bayesian inference [Sanz-Alonso et al., 2023]. A conventional approach is via the Langevin dynamics, under the assumption that V is differentiable:

$$dX_t = -\nabla V(X_t)dt + \sqrt{2}dB_t \quad (1)$$

where B_t denotes the standard Brownian motion in \mathbb{R}^d . Under suitable conditions on V , this stochastic differential equation admits π as a unique invariant distribution, and the law of X_t converges to π as $t \rightarrow \infty$ [Roberts and Tweedie, 1996]. In practice, the stochastic dynamics (1) must be discretized for implementation. A simple Euler-Maruyama scheme results in the so-called Unadjusted Langevin Algorithm (ULA)

$$X_{k+1} = X_k - \gamma \nabla V(X_k) + \sqrt{2\gamma} Z_{k+1}$$

where $\gamma > 0$ and $\{Z_k\}_k$ follows i.i.d. normal distribution.

When V is (strongly) convex, the sampling problem falls within the class of log-concave sampling, and the properties of these dynamics are well studied; see, e.g., the recent note [Chewi, 2023]. In contrast, in many practical applications [E et al., 2002, Cui et al., 2023], the target distribution may exhibit multi-peak, non-log-concave, non-log-differentiable behaviors. Beyond convexity, distant dissipativity (also known as *strong convexity at infinity*) provides a key structural condition under which convergence of these dynamics can still be established [Eberle, 2016, De Bortoli and Durmus, 2019, Johnston et al., 2025]. While the ULA is simple and easy to

*Division of Mathematical Sciences, School of Physical and Mathematical Sciences, Nanyang Technological University, Singapore. hoangph.luu@ntu.edu.sg

†Division of Mathematical Sciences, School of Physical and Mathematical Sciences, Nanyang Technological University, Singapore. zhongjian.wang@ntu.edu.sg (Corresponding)

implement, it is not universally well-suited to all problems, particularly when the potential V is ill-posed in terms of differentiability (e.g., non-differentiable or even non-Fréchet subdifferentiable). In many practical settings, however, V possesses additional structure—such as a composite form—that can be explicitly exploited to design more effective sampling algorithms. In this work, we consider nonconvex and nonsmooth potentials V that satisfy a distant dissipativity condition and admit the decomposition

$$V = f + r = f + (r_1 - r_2) \quad (2)$$

where f is L -smooth and r_1, r_2 are real-valued convex functions. The function r is called a difference-of-convex (DC) function, with r_1 and r_2 as its DC components.

The class of DC functions forms a broad and expressive subclass of nonconvex, nonsmooth functions [Pham Dinh and Le Thi, 1997, Le Thi et al., 2022, An and Tao, 2005, Nouiehed et al., 2019, Cui et al., 2018, Ahn et al., 2017]. In the context of Bayesian inference, f typically arises from the likelihood and is often L -smooth, such as $\|Ax - b\|^2$ under Gaussian noise, and the regularizer r , which can be nondifferentiable, comes from the prior¹. There are two main classes of priors: hand-crafted priors (e.g., LASSO, total variation), which are designed using domain knowledge to promote desired structural properties in the solution, and data-driven priors learned from training data using deep neural networks (e.g., U-Net [Ronneberger et al., 2015]), which are capable of capturing more complex data characteristics. In the former paradigm, nonconvex DC priors offer greater flexibility for encoding expert knowledge and have been shown to outperform convex priors in compressed sensing tasks [Yin et al., 2015, Liu and Pong, 2017, Yao and Kwok, 2018]. Hand-crafted DC priors (with *explicit* decompositions) include Laplace, log-sum penalty, Smoothly Clipped Absolute Deviation, Minimax Concave Penalty, Capped- ℓ_1 , PiL, ℓ_p^+ ($0 < p < 1$), ℓ_p^- ($p < 0$), $\ell_1 - \ell_2$, and $\ell_1 - \ell_{\sigma_p}$ [Le Thi et al., 2015, Yin et al., 2015, Luo et al., 2015, Yao and Kwok, 2018]. In the latter paradigm, data-driven DC regularizers based on the difference of two input-convex neural networks (ICNNs), named DICNNs, have been shown to generalize better than input-weakly convex neural networks [Zhang and Leong, 2025], while remaining more analyzable than general neural priors thanks to their DC structure.

In this work, we introduce and study a practical sampler named Difference-of-convex Langevin algorithm (DC-LA) that aims to sample from $\pi \propto e^{-V}$ where V is given in (2). DC-LA is essentially a forward-backward sampler whose forward-backward splitting is based on the principle of DC programming and DC algorithm [Pham Dinh and Le Thi, 1997]. We also incorporate Moreau smoothing techniques tailored to DC regularizers [Sun and Sun, 2023, Hu et al., 2024] to facilitate the analysis (detailed in Section 3). Let $\lambda > 0$ be a smoothing parameter, since r_1 and r_2 are convex, their Moreau envelopes, denoted r_1^λ, r_2^λ , are well-defined and smooth (see Subsection 2.2). DC-LA reads as

$$X_{k+1} = \text{Prox}_{\gamma r_1^\lambda} \left(X_k - \gamma \nabla f(X_k) + \gamma \nabla r_2^\lambda(X_k) + \sqrt{2\gamma} Z_{k+1} \right), \quad (3)$$

where $\gamma > 0$ is the step size and $\{Z_k\}_k$ follows i.i.d. normal distribution. As detailed in Section 3, DC-LA can be decomposed into *elementary operators*: gradient of f and proximal operators of r_1 and r_2 . Our main theoretical results are as follows: if V is distant dissipative (aka. strongly convex at infinity), r_1 is Lipschitz continuous, and r_2 is *either*

- (a) Lipschitz continuous,
- (b) differentiable whose gradient is κ -Hölder continuous for $0 < \kappa < 1$ (class $C^{1,\kappa}$),
- (c) smooth (class $C^{1,1}$) – in this case, we directly use ∇r_2 in (3),

¹The prior $p_{\text{prior}}(x) \propto e^{-r(x)}$ may be improper if the regularizer $r(x)$ does not grow sufficiently fast at infinity, which is typically the case for DC regularizers. However, when combined with the likelihood, the resulting posterior is assumed to define a valid, normalizable probability distribution.

then for any $q \in \mathbb{N}^*$, the q -Wasserstein distance between $p_{X_{k+1}}$ (law of X_{k+1}) and π is upper bounded by $O(\rho^{k\gamma}) + O(\gamma^{\frac{1}{2q}}) + O(\lambda^{\frac{1}{q}})$ where $\rho \in (0, 1)$. Here, the hidden constants in the first and second Big O's and ρ may depend on λ , and all constants depend on q . In the above result, the assumptions on r_2 form a continuum of regularity of r_2 : case (b) interpolates between the nonsmooth and smooth regimes as κ increases from 0 to 1, with case (a) corresponding to $\kappa = 0$ and case (c) corresponding to $\kappa = 1$. Our theoretical results leverage recent advances in forward-backward sampling algorithms [Renaud et al., 2025a], which we tailor and revise for the DC setting. See the first paragraph in the **Related Work** section for a detailed discussion. To our knowledge, DC-LA handles non-weakly convex DC regularizers (e.g., $\ell_1 - \ell_2$ and DCINNs), for which no prior *Langevin-type* convergence guarantees existed.

Contributions We study the sampling problem with the nonsmooth DC potential V , as defined in (2). We propose a forward-backward style algorithm termed DC-LA and establish its convergence to π in terms of the q -Wasserstein distance—up to discretization and smoothing errors—for all $q \in \mathbb{N}^*$ under a distant dissipativity condition on V . Numerical experiments demonstrate the merit of DC-LA, showing that it produces faithful empirical distributions in synthetic experiments and reliably provides uncertainty quantification in a real-world computed tomography application.

Related work

Euclidean forward-backward samplers ² For the composite structure of $V = f + r$, the following forward-backward scheme, named Proximal Stochastic Gradient Langevin Algorithm (PSGLA)

$$X_{k+1} = \text{Prox}_{\gamma r} \left(X_k - \gamma \nabla f(X_k) + \sqrt{2\gamma} Z_{k+1} \right) \quad (4)$$

is a natural choice. When both f and r are convex, convergence of PSGLA and its variants was studied thoroughly, for example, in [Durmus et al., 2019, Salim and Richtarik, 2020, Salim et al., 2019, Ehrhardt et al., 2024]. Recently, Renaud et al. [2025a] studied the case where f is L -smooth and r is *weakly convex* ³, and established for the first time convergence in q -Wasserstein distance ($q \in \mathbb{N}^*$) of PSGLA to π (up to discretization error), assuming convex at infinity (distant dissipativity). To be specific, they derived $W_q(p_{X_k}, \nu_\gamma) = O(\rho^{k\gamma} + \gamma^{\frac{1}{2q}})$ where $\rho \in (0, 1)$ and ν_γ satisfies $\lim_{\gamma \rightarrow 0} W_q(\nu_\gamma, \pi) = 0$ and $W_q(\nu_\gamma, \pi) = O(\gamma^{\frac{1}{q}})$ if r is further assumed to be Lipschitz continuous. We note that a weakly convex function r is a DC function whose second DC component is $r_2 = \frac{\eta}{2} \|\cdot\|^2$ for some $\eta > 0$. The converse, however, does not hold in general, for instance, several DC regularizers used in compressed sensing—such as $\ell_1 - \ell_2$ [Yin et al., 2015, Lou and Yan, 2018], $\ell_1 - \ell_{\sigma_q}$ [Luo et al., 2015], Capped ℓ_1 [Zhang, 2010b], and DCINNs with leaky ReLU activations [Zhang and Leong, 2025]—are *not* weakly convex (see Appendix F), yet are widely used in image and signal reconstruction because they better model (gradient) sparsity and yield higher reconstruction quality than convex counterparts. Furthermore, while the assumption of convexity at infinity is quite a minimal assumption if one seeks convergence to π , their analysis ultimately relies on an overly strict convexity condition on r at infinity. Loosely speaking, Assumption 3 in [Renaud et al., 2025a] requires the convex modulus at infinity of r (formally its Moreau envelope r^γ) to dominate four times of the Lipschitz smoothness constant (defined over some proximal region) of r . This requirement is rather unrealistic, since one would naturally expect the latter to dominate the former instead. Indeed, in Appendix E we argue that this assumption is *impossible* to satisfy. That said, their work provides important stability results (Subsection 2.4) and lays the foundation for our work. In another work tackling nonconvex,

²Here, “Euclidean” refers to the algorithmic design rather than the geometric nature of the underlying flow.

³A function r is called η weakly convex ($\eta > 0$) if $r + \frac{\eta}{2} \|\cdot\|^2$ is convex.

nonsmooth potentials, [Luu et al. \[2021\]](#) also studied forward-backward schemes leveraging on the Moreau envelope. However, their results only established consistent guarantees for the schemes without quantifying convergence to the target distribution.

Wasserstein forward-backward samplers On a different front, where forward-backward schemes are designed directly in the Wasserstein space, [Salim et al. \[2020\]](#) studied a Wasserstein proximal algorithm in the convex setting, and [Luu et al. \[2024\]](#) extended the scheme to DC settings. In contrast to our approach, where (Euclidean) proximal operators are often available in closed form, the Wasserstein proximal operators lack closed-form expressions and must instead be approximated, e.g., by neural networks [\[Mokrov et al., 2021, Luu et al., 2024\]](#). When restricting to Gaussian distributions, the Wasserstein proximal operator admits a closed-form expression, whereas computing the Bures–Wasserstein gradient in the forward step relies on Monte Carlo estimation or variance-reduction techniques [\[Diao et al., 2023, Luu et al., 2025\]](#).

Gibbs samplers for composite structures Composite structures can also be handled by Gibbs samplers, which decompose a complicated sampling problem into simpler sampling subproblems [\[Sorensen et al., 1995, Geman and Geman, 1984\]](#). Recently, [Sun et al. \[2024\]](#) established first-order stationary convergence guarantees (in terms of Fisher information) for Gibbs sampling in the nonconvex setting.

2 Preliminary

2.1 Lipschitz and distant dissipativity

A function f is called Lipschitz continuous (or M -Lipschitz for some $M > 0$) if $|f(x) - f(y)| \leq M\|x - y\|$ for all $x, y \in \mathbb{R}^d$. f is called Lipschitz-smooth (or L_f -smooth for some $L_f > 0$) if

$$\|\nabla f(x) - \nabla f(y)\| \leq L_f\|x - y\|, \quad \forall x, y \in \mathbb{R}^d.$$

while it is said to have (θ, M) -Hölder continuous gradient if

$$\|\nabla f(x) - \nabla f(y)\| \leq M\|x - y\|^\theta, \quad \forall x, y \in \mathbb{R}^d.$$

Given a drift $b : \mathbb{R}^d \rightarrow \mathbb{R}^d$, we say that b is distant dissipative (or weak dissipative) [\[Mou et al., 2022, Debussche et al., 2011\]](#) if there exist $R \geq 0$ and $m > 0$ such that $\forall x, y \in \mathbb{R}^d$ satisfying $\|x - y\| \geq R$,

$$\langle b(x) - b(y), x - y \rangle \geq m\|x - y\|^2. \quad (5)$$

b is also called (m, R) -distant dissipative. If $b = \nabla V$ for some V , by abusing of terminology, we also say that V is distant dissipative. In our work, as V is not differentiable, we may extend the concept to some generalized notion of gradients (Section 3). Note that a strongly convex function is dissipative, i.e., (5) holds for all $x, y \in \mathbb{R}^d$.

2.2 Moreau envelope and proximal operator

Given a convex function g and $\lambda > 0$, we denote the Moreau envelope g^λ of g as

$$g^\lambda(x) = \inf_y \left\{ g(y) + \frac{1}{2\lambda}\|x - y\|^2 \right\}$$

and the proximal operator of g as

$$\text{Prox}_{\lambda g}(x) = \arg\min_y \left\{ g(y) + \frac{1}{2\lambda}\|x - y\|^2 \right\}.$$

Note that, in this paper, we only work with Moreau envelopes and proximal operators of convex functions. In the following lemma, we summarize some known important properties of the Moreau envelope and the proximal operator [Bauschke and Combettes, 2020] that are used throughout this paper.

Lemma 1. *Let g be a convex function and $\lambda > 0$. The following properties hold*

- (i) g^λ is convex, $\frac{1}{\lambda}$ -smooth, and is a lower bound of g , i.e., $g^\lambda(x) \leq g(x)$, $\forall x \in \mathbb{R}^d$. Furthermore, if g is G -Lipschitz, $g(x) \leq g^\lambda(x) + \frac{G^2\lambda}{2}$, $\forall x \in \mathbb{R}^d$.
- (ii) $\nabla g^\lambda(x) = \frac{1}{\lambda}(x - \text{Prox}_{\lambda g}(x))$.
- (iii) $\text{Prox}_{\lambda g}$ is nonexpansive, i.e., for all $x, y \in \mathbb{R}^d$, $\|\text{Prox}_{\lambda g}(x) - \text{Prox}_{\lambda g}(y)\| \leq \|x - y\|$.
- (iv) $\nabla g^\lambda(x) \in \partial g(\text{Prox}_{\lambda g}(x))$ where ∂g denotes the usual convex subdifferential of g .

2.3 q -Wasserstein distance

Given a measurable map $\varphi : \mathbb{R}^d \rightarrow \mathbb{R}^d$ and a probability measure μ , the pushforward measure $\varphi_\# \mu$ is defined by $(\varphi_\# \mu)(A) = \mu(\varphi^{-1}(A))$ for all measurable sets A .

For $q \geq 1$, let $\mathcal{P}_q(\mathbb{R}^d)$ denote the set of probability distributions over \mathbb{R}^d that have finite q -th moment: $\mu \in \mathcal{P}_q(\mathbb{R}^d)$ iff $\int \|x\|^q d\mu(x) < +\infty$. Let $\mu, \nu \in \mathcal{P}_q(\mathbb{R}^d)$, the q -Wasserstein distance [Villani et al., 2008, Ambrosio et al., 2005] between μ and ν is

$$W_q(\mu, \nu) = \left(\min_{\xi \in \Gamma(\mu, \nu)} \int_{\mathbb{R}^d \times \mathbb{R}^d} \|x - y\|^q d\xi(x, y) \right)^{\frac{1}{q}}$$

where $\Gamma(\mu, \nu)$ is the set of probability distributions over $\mathbb{R}^d \times \mathbb{R}^d$ whose marginals are μ and ν .

2.4 Langevin dynamics with general drifts

In the definition of the ULA, one may, in practice, replace the exact gradient ∇V with an approximate drift b , provided that b remains close to ∇V [Rásonyi and Tikosi, 2022],

$$X_{k+1} = X_k - \gamma b(X_k) + \sqrt{2\gamma} Z_{k+1}. \quad (6)$$

Stability results are to establish (quantitative) bounds on the distance (e.g. Wasserstein) between the invariant distribution of ULA and the invariant distribution of (6) based on the distance between b and ∇V (e.g., some L_2 norm). More generally, given two general drifts b^1 and b^2 , it is desirable to bound the discrepancy between the invariant distributions of two processes by $\|b^1 - b^2\|_{L_2}$. Note that the step size γ also influences the invariant distribution, as different values of γ lead to different limiting laws. Under suitable conditions, let π_γ^1 and π_γ^2 denote the invariant distributions of the processes with drifts b^1 and b^2 , respectively. It is established in [Renaud et al., 2023] that, under certain conditions, $W_1(\pi_\gamma^1, \pi_\gamma^2) = O(\|b^1 - b^2\|_{L_2(\pi_\gamma^1)}^{\frac{1}{2}}) + O(\gamma^{\frac{1}{8}})$ and latter refined and generalized in [Renaud et al., 2025a] to $W_q(\pi_\gamma^1, \pi_\gamma^2) = O(\|b^1 - b^2\|_{L_2(\pi_\gamma^1)}^{\frac{1}{q}})$ for $q \in \mathbb{N}^*$. The latter result shows that discretization errors do not accumulate along the processes. Similar ergodic results were also established earlier in compact domains, see [Wang et al., 2021, Ferré and Stoltz, 2019].

3 Proximal Langevin algorithm with DC regularizers

Recall the target distribution $\pi \propto e^{-V}$ and $V = f + r$ where f is Lipschitz smooth and r is DC.

Assumption 1. f is L_f -smooth and $r = r_1 - r_2$ where $r_1, r_2 : \mathbb{R}^d \rightarrow \mathbb{R}$ are convex functions.

We next impose a *distant dissipativity* condition on V . Unlike strong convexity, this assumption requires the gradient field of V to be dissipative only when x and y are sufficiently far apart [Eberle, 2016, Eberle and Majka, 2019].

Assumption 2 (Distant dissipative V). *There exist $R_0 \geq 0, \mu > 0$ such that $\forall x, y \in \mathbb{R}^d$ with $\|x - y\| \geq R_0$,*

$$\langle \nabla f(x) + u_1 - u_2 - \nabla f(y) - v_1 + v_2, x - y \rangle \geq \mu \|x - y\|^2, \quad (7)$$

$$\forall u_1 \in \partial r_1(x), u_2 \in \partial r_2(x), v_1 \in \partial r_1(y), v_2 \in \partial r_2(y).$$

Distant dissipativity (7) implies that V exhibits quadratic growth and consequently $\pi \propto e^{-V}$ has sub-Gaussian tails (Appendix A).

Difference of Moreau envelopes Now we want to apply a forward-backward Langevin-type algorithm to V . Thanks to the DC structure of r , the principle of DC programming and DC algorithm [Pham Dinh and Le Thi, 1997] suggests that the forward step should apply to $f - r_2$ while the backward step should apply to r_1 for tractability and robustness. To retain a degree of smoothness in the forward step, we replace r_2 with its Moreau envelope r_2^λ . This modification is necessary, as the concavity of $-r_2$ and its associated tangent inequality are hardly sufficient to guarantee the stability results and to enable two-sided comparisons of general drifts (Subsection 4.1). On the other hand, the analysis in [Renaud et al., 2025a] suggests that, if the backward step is applied to r_1 , r_1 should be smooth on the set $\text{Prox}_{\gamma r_1}(\mathbb{R}^d) := \{\text{Prox}_{\gamma r_1}(x) : x \in \mathbb{R}^d\}$, where γ is the step size. This requirement arises in order to prevent the Lipschitz smoothness constant of r_1^γ to explode as $\gamma \rightarrow 0$. In our setting, $\text{Prox}_{\gamma r_1}(\mathbb{R}^d) = \mathbb{R}^d$ [Hiriart-Urruty, 2024, Fact 2], and r_1 remains nonsmooth on \mathbb{R}^d , so this requirement cannot be satisfied. To circumvent this issue, we further replace r_1 with its Moreau envelope r_1^λ . These considerations motivate the following augmented potential and distribution

$$V_\lambda = (f - r_2^\lambda) + r_1^\lambda, \quad \pi_\lambda \propto e^{-V_\lambda}, \quad (8)$$

which results in the DC-LA (3).

Remark 2. *The difference-of-convex structure of $r = r_1 - r_2$ allows this Moreau envelope approximation, rather than applying one Moreau envelope to the entire r which is generally an ill-posed object (e.g., multi-valued and discontinuous, see Appendix G). This kind difference-of-Moreau-envelope has been used in the optimization literature [Sun and Sun, 2023, Hu et al., 2024].*

Remark 3. *In practice, there is also a class of sparsity promoting DC regularizers where r_2 is Lipschitz smooth [Yao and Kwok, 2018]. In such a case, we do not need to smooth out r_2 . We consider this case in Subsection 4.2.*

We impose the following assumption on r_1 .

Assumption 3. *There exists $G_1 > 0$ such that $\forall x \in \mathbb{R}^d, \forall z \in \partial r_1(x)$, it holds $\|z\| \leq G_1$.*

To be noted, Assumption 3 is equivalent to r_1 being G_1 -Lipschitz continuous. In Appendix D, we show that this assumption holds for commonly-used DC regularizers.

Unrolled DC-LA For a fixed $\lambda > 0$, starting from some initial distribution $X_0 \sim p_0$, DC-LA (3) with step size $\gamma > 0$ can be rewritten as follows

$$\begin{aligned} Y_{k+1} &= X_k - \gamma \nabla f(X_k) + \gamma \nabla r_2^\lambda(X_k) + \sqrt{2\gamma} Z_{k+1} \\ X_{k+1} &= \text{Prox}_{\gamma r_1^\lambda}(Y_{k+1}). \end{aligned} \quad (\text{DC-LA})$$

Since $\nabla r_2^\lambda(x) = (1/\lambda)(x - \text{Prox}_{\lambda r_2}(x))$, Y_{k+1} becomes

$$Y_{k+1} = \frac{\lambda + \gamma}{\lambda} X_k - \gamma \nabla f(X_k) - \frac{\gamma}{\lambda} \text{Prox}_{\lambda r_2}(X_k) + \sqrt{2\gamma} Z_{k+1}. \quad (9)$$

To compute X_{k+1} , we use the identity (Lemma 10 in the appendix) connecting the proximal operator of the Moreau envelope to the proximal operator of r_1 :

$$X_{k+1} = \frac{1}{\gamma + \lambda} \left(\gamma \text{Prox}_{(\gamma + \lambda)r_1}(Y_{k+1}) + \lambda Y_{k+1} \right). \quad (10)$$

Now DC-LA has been decomposed into elementary operators (also see Appendix C for a complete unroll). For the analysis of DC-LA in the next section, we work directly with ∇r_2^λ and $\text{Prox}_{\gamma r_1^\lambda}(x)$ for convenience.

4 Convergence Analysis of DC-LA

We begin with a convergence analysis in the general setting where both r_1 and r_2 are nonsmooth in Section 4.1. We then specialize to the case where r_2 is smooth and no longer needs to be regularized by Moreau envelope in Section 4.2.

4.1 Nonsmooth r_2

We impose the following assumption on r_2 .

Assumption 4. r_2 satisfies one of the followings:

- (i) There exists $G_2 > 0$ such that $\forall x \in \mathbb{R}^d, \forall z \in \partial r_2(x)$, it holds $\|z\| \leq G_2$.
- (ii) r_2 is differentiable whose gradient is (κ, M) -Hölder continuous with $\kappa \in (0, 1)$ and $M > 0$.

To be noted that Assumption 4(i) is satisfied by $\ell_1 - \ell_2$ [Yin et al., 2015], $\ell_1 - \ell_{\sigma_q}$ [Luo et al., 2015], capped ℓ_1 [Zhang, 2010b], and PiL [Le Thi et al., 2015], while Assumption 4(ii) holds, for example, for $\ell_1 - \ell_2^p$ with $p \in (1, 2)$, see Appendix D.

The following lemma (proved in Appendix I.1) provides a more concrete characterization of the distant dissipativity of V under Assumption 4.

Lemma 4. Under Assumptions 1, 3 and 4, V is distant dissipative (7) iff f is distant dissipative.

We first analyze the sequence $\{Y_k\}_k$ of DC-LA. Similar to [Renaud et al., 2025a], we have the following lemma whose proof is in Appendix I.2.

Lemma 5. $\{Y_k\}_k$ is an instance of the general ULA,

$$Y_{k+1} = Y_k - \gamma b_\lambda^\gamma(Y_k) + \sqrt{2\gamma} Z_{k+1} \quad (11)$$

where the drift is $b_\lambda^\gamma(y) := \nabla r_1^\lambda(\text{Prox}_{\gamma r_1^\lambda}(y)) + \nabla f(\text{Prox}_{\gamma r_1^\lambda}(y)) - \nabla r_2^\lambda(\text{Prox}_{\gamma r_1^\lambda}(y))$. Furthermore, b_λ^γ is $(\frac{2}{\lambda} + L_f)$ -Lipschitz.

In the following lemma whose proof is in Appendix I.3, we show that b_λ^γ is distant dissipative.

Lemma 6. Let $\gamma_0 > 0$. Under Assumptions 1, 2, 3, 4, for all $\gamma \in (0, \gamma_0]$, and x, y satisfying the distance condition: $\|x - y\| \geq \max \left\{ R_0, \frac{8G_1 + 4L_f \gamma_0 G_1 + 4G_2}{\mu} \right\}$ if Assumption 4(i); $\|x - y\| \geq \max \left\{ R_0, \frac{16G_1 + 8L_f \gamma_0 G_1}{\mu}, \left(\frac{4M}{\mu} \right)^{\frac{1}{1-\kappa}} \right\}$ if Assumption 4(ii), it holds

$$\langle b_\lambda^\gamma(x) - b_\lambda^\gamma(y), x - y \rangle \geq \frac{\mu}{2} \|x - y\|^2$$

where G_1 is given in Assumption 3, R_0, μ are given in Assumption 2, and G_2, M, κ are given in Assumption 4.

We next define another drift

$$\bar{b}_\lambda^\gamma(y) = \nabla r_1^\lambda(\text{Prox}_{\gamma r_1^\lambda}(y)) + \nabla f(y) - \nabla r_2^\lambda(y), \quad (12)$$

and the corresponding unadjusted Langevin algorithm:

$$\bar{Y}_{k+1} = \bar{Y}_k - \gamma \bar{b}_\lambda^\gamma(\bar{Y}_k) + \sqrt{2\gamma} \bar{Z}_{k+1}, \quad (13)$$

with $\bar{Y}_1 \sim Y_1$. We also denote

$$\pi_{\lambda, \gamma}(x) \propto \exp(-f(x) - (r_1^\lambda)^\gamma(x) + r_2^\lambda(x)) \quad (14)$$

and

$$\nu_{\lambda, \gamma} = (\text{Prox}_{\gamma r_1^\lambda})_\# \pi_{\lambda, \gamma}. \quad (15)$$

Note that $-\nabla \log \pi_{\lambda, \gamma} = \bar{b}_\lambda^\gamma$. In a similar manner, we can show that: for all $\gamma > 0$, \bar{b}_λ^γ is $(\frac{2}{\lambda} + L_f)$ -Lipschitz; and for all $\lambda > 0$, for all $\gamma > 0$, $\langle \bar{b}_\lambda^\gamma(x) - \bar{b}_\lambda^\gamma(y), x - y \rangle \geq \frac{\mu}{2} \|x - y\|^2$ whenever $\|x - y\| \geq \max \left\{ R_0, \frac{8G_1 + 4G_2}{\mu} \right\}$ if Assumption 4(i); $\|x - y\| \geq \max \left\{ R_0, \frac{16G_1}{\mu}, \left(\frac{4M}{\mu} \right)^{\frac{1}{1-\kappa}} \right\}$ if Assumption 4(ii). For completeness, we provide proof in Appendix I.4.

Based on the Lipschitz smoothness and distant dissipativity of these general drifts, the stability results from [Renaud et al., 2025a] apply. Leveraging these results, we derive Theorem 7 that quantifies the Wasserstein distance between the distributions of iterates $\{Y_k\}_k$ (resp. $\{X_k\}_k$) of DC-LA and $\pi_{\lambda, \gamma}$ (resp. $\nu_{\lambda, \gamma}$). Detailed proof is in Appendix I.5.

Theorem 7. Let $q \in \mathbb{N}^*$ and $\lambda > 0$, under Assumptions 1, 2, 3, 4, for $\{(X_k, Y_k)\}_k$ being DC-LA's sequence starting from X_0 with $\mathbb{E}\|X_0\| < +\infty$ if $q = 1$ and $\mathbb{E}\|X_0\|^{2q} < +\infty$ if $q \geq 2$. Let γ satisfy: $\gamma \leq \frac{\mu\lambda^2}{2(2+\lambda L_f)^2}$ if $q = 1$ and $\gamma \leq \min \left\{ \frac{\mu\lambda^2}{(2+\lambda L_f)^2 2^{2q+3}(2q-1)}, \frac{\lambda}{4(2+\lambda L_f)} \right\}$ if $q \geq 2$. There exist $A_\lambda, B_\lambda > 0$ and $\rho_\lambda \in (0, 1)$ such that

$$W_q(p_{X_{k+1}}, \nu_{\lambda, \gamma}) \leq W_q(p_{Y_{k+1}}, \pi_{\lambda, \gamma}) \leq A_\lambda \rho_\lambda^{k\gamma} + B_\lambda \gamma^{\frac{1}{2q}}$$

where $\pi_{\lambda, \gamma}$ and $\nu_{\lambda, \gamma}$ are defined in (14) and (15).

The dependence of $A_\lambda, B_\lambda, \rho_\lambda$ to λ is discussed in Appendix I.6 for the case $q = 1$ for simplicity.

Finally, we quantify $W_q(\pi_{\lambda, \gamma}, \pi_\lambda)$ and $W_q(\pi_\lambda, \pi)$. Since $\nabla r_1^\lambda(x) \in \partial r_1(\text{Prox}_{\lambda r_1}(x))$, under Assumption 3, $\|\nabla r_1^\lambda(x)\| \leq G_1$ for all x , meaning that r_1^λ is G_1 -Lipschitz continuous. Applying [Renaud et al., 2025a, Proposition 1], $W_q(\pi_{\lambda, \gamma}, \pi_\lambda) = O(\gamma^{1/q})$ and $W_q(\nu_{\lambda, \gamma}, \pi_\lambda) = O(\gamma^{1/q})$ ⁴. Under the Assumption 4, we show in Appendix I.7 that: $W_q(\pi_\lambda, \pi) = O(\lambda^{1/q})$. Putting these bounds together, we derive the following bound.

⁴We remove the condition $\gamma \leq 2/G_1^2$ in [Renaud et al., 2025a, Proposition 1] for simplicity.

Theorem 8. Let $q \in \mathbb{N}^*$, under Assumptions 1, 2, 3, 4, for $0 < \lambda \leq \lambda_0$ for some $\lambda_0 > 0$, let $\{X_k\}$ be the DC-LA's sequence starting from X_0 with $\mathbb{E}\|X_0\| < +\infty$ if $q = 1$ and $\mathbb{E}\|X_0\|^{2q} < +\infty$ if $q \geq 2$. For γ satisfying the condition as in Theorem 7, there exist $A_\lambda, B_\lambda, C > 0$ and $\rho_\lambda \in (0, 1)$,

$$W_q(p_{X_{k+1}}, \pi) \leq A_\lambda \rho_\lambda^{k\gamma} + B_\lambda \gamma^{\frac{1}{2q}} + C \lambda^{\frac{1}{q}}.$$

In Theorem 8, the bound converges to zero in a stage-wise fashion. The third term scales as $O(\lambda^{1/q})$. With λ fixed, the second term scales as $O(\gamma^{1/(2q)})$. When both λ and γ are fixed, the first term vanishes with k .

4.2 Smooth r_2

Yao and Kwok [2018] identified a structured family of DC regularizers with a Lipschitz continuous first component and a smooth second component, consisting of the Geman penalty [Geman and Yang, 1995], log-sum penalty [Candes et al., 2008], Laplace [Trzasko and Manduca, 2008], Minimax Concave Penalty [Zhang, 2010a], and Smoothly Clipped Absolute Deviation [Fan and Li, 2001]. When r_2 has some smoothness, we only need to approximate r_1 by its Moreau envelope, resulting in the augmented potential $V_\lambda = f - r_2 + r_1^\lambda$ and the corresponding scheme named DC-LA-S(implified)

$$\begin{aligned} Y_{k+1} &= X_k - \gamma \nabla f(X_k) + \gamma \nabla r_2(X_k) + \sqrt{2\gamma} Z_{k+1} \\ X_{k+1} &= \text{Prox}_{\gamma r_1^\lambda}(Y_{k+1}). \end{aligned} \quad (16)$$

By applying a similar analysis in the general case, we obtain Theorem 9. Proof is given in Appendix I.8.

Theorem 9. Let $q \in \mathbb{N}^*$. Under Assumptions 1, 2, 3, and r_2 being L_{r_2} -smooth, for $\lambda > 0$, let $\{X_k\}$ be DC-LA-S's sequence starting from X_0 with $\mathbb{E}\|X_0\| < +\infty$ if $q = 1$ and $\mathbb{E}\|X_0\|^{2q} < +\infty$ if $q \geq 2$. Let γ satisfy: $\gamma \leq \frac{\mu\lambda^2}{2(1+\lambda L_f + \lambda L_{r_2})^2}$ if $q = 1$ and

$$\gamma \leq \min \left\{ \frac{\mu\lambda^2}{(1+\lambda L_f + \lambda L_{r_2})^2 2^{2q+3}(2q-1)}, \frac{\lambda}{4(1+\lambda L_f + \lambda L_{r_2})} \right\}$$

if $q \geq 2$. There exist $A_\lambda, B_\lambda, C > 0$ and $\rho_\lambda \in (0, 1)$ such that

$$W_q(p_{X_{k+1}}, \pi) \leq A_\lambda \rho_\lambda^{k\gamma} + B_\lambda \gamma^{\frac{1}{2q}} + C \lambda^{\frac{1}{q}}.$$

5 Experiments

We study sampling problems using an $\ell_1 - \ell_2$ prior [Yin et al., 2015] on synthetic data (Gaussian likelihoods with varying means and covariance matrices) in a 2D setting to enable density visualization in Subsection 5.1, and a DCINNs prior [Zhang and Leong, 2025] on real Computed Tomography data of size 512×512 in Subsection 5.2. See Appendix J for additional experiments and details.⁵

5.1 $\ell_1 - \ell_2$ prior

We consider the potential of the form $V(x) = f(x) + \tau(\|x\|_1 - \|x\|_2)$ where $f(x) = \frac{1}{2}(x - \mu)^\top \Sigma(x - \mu)$ for some $\Sigma \succ 0$ and $\tau > 0$ controlling the sparsity level. The proximal operators of $\|\cdot\|_1$ and $\|\cdot\|_2$ are available in closed-form, known as soft thresholding operator and block soft thresholding operator, respectively (Appendix J). Furthermore, both $\|\cdot\|_1$ and $\|\cdot\|_2$ are Lipschitz and Lemma 4 applies, implying that V is distant dissipative.

⁵Our code is at <https://github.com/MCS-hub/DC-LA26>.

Baselines Since r is not weakly convex, PSGLA does not come with convergence guarantees. Nevertheless, because the proximal operator of r admits a closed-form expression [Lou and Yan, 2018], we include a comparison of our scheme against PSGLA. For reference, we also run ULA on both the nonsmooth potential V and its smoothed surrogate V_λ , the latter referred to as Moreau ULA.

Setups For the target distribution, we set $\tau = 10$, $\Sigma = \begin{bmatrix} 1 & 0.8 \\ 0.8 & 1 \end{bmatrix}$, $\mu \in \{[0, 0]^\top, [1, 1]^\top, [2, 2]^\top\}$. For the augmented potential V_λ , we set $\lambda = 0.01$. Although our theoretical analysis provides a sufficient condition on the stepsize γ for convergence of DC-LA, in this experiment, we fix a common step size $\gamma = 0.005$ for all methods across all datasets. This value yields stable behavior and reasonable mixing for three algorithms and is used as a neutral default rather than a performance-optimized choice. For each algorithm, we run 5000 chains of length 1000 and keep the last samples. In Appendix J.2, we conduct an **ablation study** on (λ, γ) , suggesting DC-LA is relatively robust.

Results Figure 1 shows the target density (the normalizing constant is computed by `dblquad` from `scipy`⁶) and histograms of samples produced by the sampling algorithms. The effect of $\ell_1 - \ell_2$ prior can be seen clearly as it highlights coordinate axes, promoting sparsity. DC-LA faithfully captures the target density. On the other hand, ULA and Moreau ULA are blurry, while PSGLA is the sharpest but appears to overemphasize the coordinates. We compute the binned KL divergence⁷ between the histograms produced by each sampling method and the binned target distribution using identical bins, and Figure 2 shows that DC-LA achieves the lowest KL divergence across bin resolutions.

5.2 Computed Tomography with DICNNs priors

We consider a Computed Tomography (CT) experiment using the Mayo Clinic’s human abdominal CT scans [Moen et al., 2021], each of size 512×512 . Given a ground truth CT scan x^* , the forward model is $y = Ax^* + \epsilon$ where $\epsilon \sim \mathcal{N}(0, \sigma^2 I)$ and A is the data acquisition using a 2D parallel-beam ray transform implemented in ODL [Adler et al., 2017] with 350 uniform projections collected from 0° to 120° . We use the data-driven DC prior based on the difference of two input-convex neural networks (ICNNs) proposed in [Zhang and Leong, 2025]. The target distribution is of the form $\pi(x) \propto \exp\left(-\frac{1}{2\sigma^2}\|y - Ax\|^2 - \tau(\text{NN}_1(\theta_1^*, x) - \text{NN}_2(\theta_2^*, x))\right)$ where NN_1, NN_2 are two ICNNs with pretrained parameters θ_1^*, θ_2^* . The experiment is conditioned on σ , i.e., treating σ as a known parameter. The DC regularizer $r(\theta, x) = \text{NN}_1(\theta_1, x) - \text{NN}_2(\theta_2, x)$ was trained using the adversarial regularization framework [Lunz et al., 2018] encouraging it to be Lipschitz. Therefore, we largely assume that each of its components is also Lipschitz. On the other hand, as A is in general ill-conditioned, Lemma 4 does not apply directly. We can slightly augment f to confine it at infinity. For example, we can add to f a radial part $\phi(\|x\|)$, where $\phi(r) \approx 0$ for $r \leq R$ and $\phi(r) \approx (r - R)^2$ for $r > R$ with R sufficiently large to preserve the main posterior mass. Nevertheless, in this study, we leave the likelihood as-is.

Setups We set $\sigma = 0.2$, $\tau = \hat{\lambda}/\sigma^2$ where $\hat{\lambda} = \|A^*(Ax_{val} - y_{val})\|$ with one validation data point (x_{val}, y_{val}) . For DC-LA, the proximal operators of NN_1 and NN_2 are not in closed-form. For a given $\eta > 0$, let $v^* = \text{Prox}_{\eta \text{NN}_i}(x)$, v^* solves the fixed-point equation: $v^* \in x - \eta \partial \text{NN}_i(v^*)$, we apply several fixed-point iterations: $v := x - \eta \partial \text{NN}_i(v)$. In practice, we found that 1 iteration is sufficient, and we use it for both proximal operators. Note that Ehrhardt et al. [2024] suggested that bounded approximation errors in computing proximal operators lead to controlled bias;

⁶<https://docs.scipy.org/doc/scipy/reference/generated/scipy.integrate.dblquad.html>

⁷In this scenario, the Wasserstein distance is difficult to evaluate due to the absence of true samples from the target distribution.

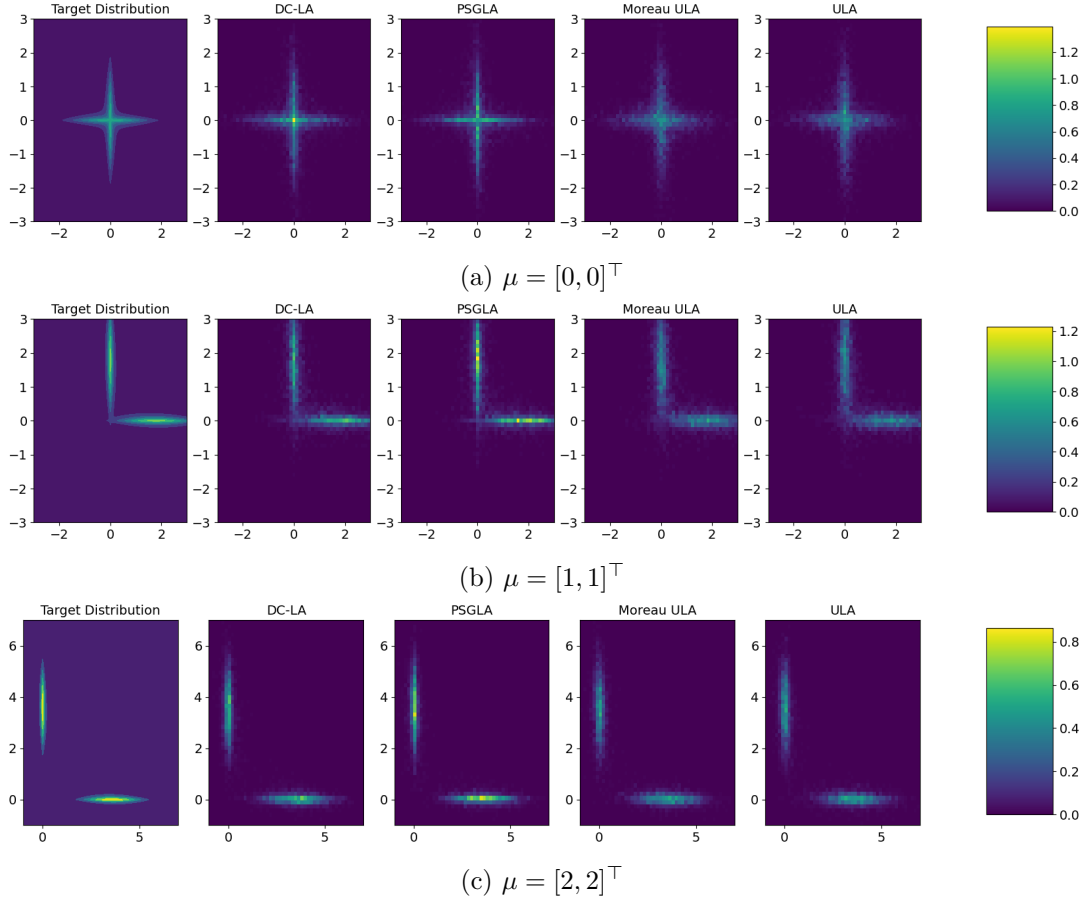


Figure 1: Target density and histograms of samples produced by ULA, Moreau ULA, PSGLA and DC-LA

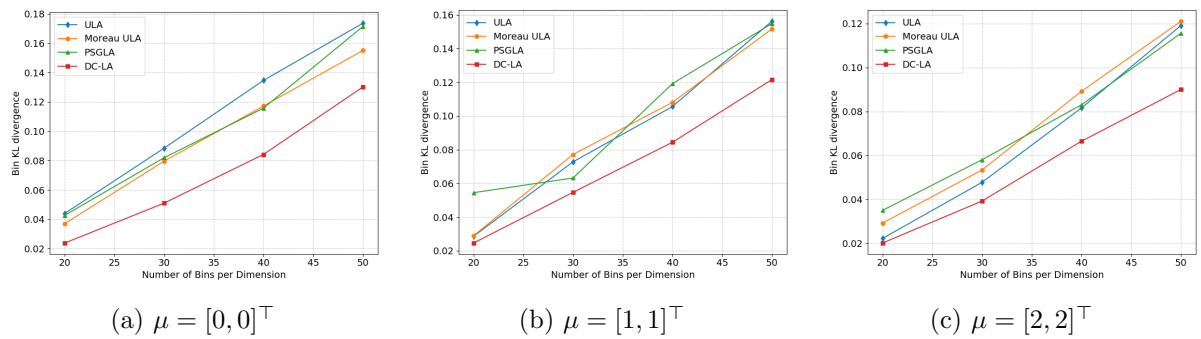


Figure 2: Binned KL divergences between samples from ULA, Moreau ULA, PSGLA, and DC-LA and the target distributions

extending our analysis to this setting is a promising direction for future work. The step size of DC-LA is $\gamma = 10^{-5}\sigma^2$ and the smoothing parameter $\lambda = 10^{-4}$. We simulate 100 Markov chains, each of length 2000, initialized from a black image and retaining only the final sample from each chain. We also compute the MAP estimate by iterating $x_{k+1} = \text{Prox}_{\gamma r_1}(x_k - \gamma \nabla f(x_k) + \eta \partial r_2(x_k))$ (called PSM – Proximal Subgradient Method [Zhang and Leong, 2025]), which is the optimization counterpart of DC-LA. The optimizer runs for up to 20,000 iterations.

Results In Figure 3 (more results are give in Appendix J.3), panel (a) shows the ground-truth image, panel (b) presents the posterior mean produced by DC-LA, panel (c) shows the estimated pixel-wise posterior variance produced by DC-LA, while panels (d), (e), (f) show the MAP reconstructions produced by PSM at iterations 2000, 10000, 20000 iterations. The posterior mean successfully recovers the overall anatomical structures. It achieves higher SSIM (Structural Similarity Index Measure) and PSNR (Peak Signal-to-Noise Ratio)⁸ than the MAP estimate obtained by PSM at 2,000 iterations, which matches the length of the DC-LA chains, although the posterior mean averages over 100 parallel chains. At 10,000 iterations, PSM roughly matches the performance of DC-LA. We run the PSM until the 20,000 iterations, when it slightly surpasses DC-LA. From the PSNR, we observe that the PSM’s performance effectively saturates and even decreases between 10,000 and 20,000 iterations. Meanwhile, the posterior variance produced by DC-LA highlights regions of higher uncertainty, primarily around boundaries and fine textures, indicating where the reconstruction is less confident. In contrast, large homogeneous regions exhibit small variance, implying agreement between the likelihood and prior in these regions. However, the samples miss a small structure in the lower-left region, and the posterior variance does not highlight this area, suggesting either that the samples are not sufficiently representative of the posterior or that the posterior itself is overconfident in this region.

6 Conclusion

We propose a mathematically justified sampler DC-LA for nonsmooth DC regularizers, extending beyond log-concave settings and ensuring convergence under distant dissipativity. Our work overcomes the limitations of the assumptions in [Renaud et al., 2025a] while considering DC regularizers that are not necessarily weakly convex. DC-LA is able to produce sensible variance images in a computed tomography application with DICNN priors—an aspect largely overlooked by existing work in this domain, which typically focuses solely on MAP estimation. Future work will explore the practical use of these variance images in downstream applications, e.g., [Jun et al., 2025].

Acknowledgments

The authors thank Marien Renaud for the helpful discussion, Yasi Zhang for providing the pretrained parameters of the DICNNs, and the funding support from NTU-SUG and MOE AcRF Tier 1 RG17/24.

References

Jonas Adler, Holger Kohr, and Ozan Öktem. Operator discretization library (ODL). *Zenodo*, 2017.

Miju Ahn, Jong-Shi Pang, and Jack Xin. Difference-of-convex learning: directional stationarity, optimality, and sparsity. *SIAM Journal on Optimization*, 27(3):1637–1665, 2017.

⁸SSIM, PSNR: higher is better

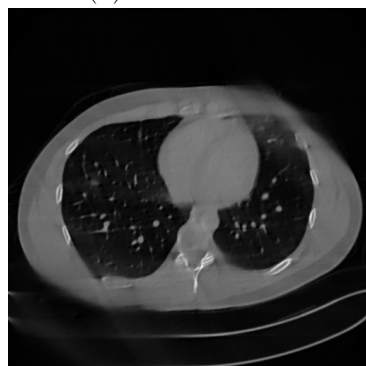
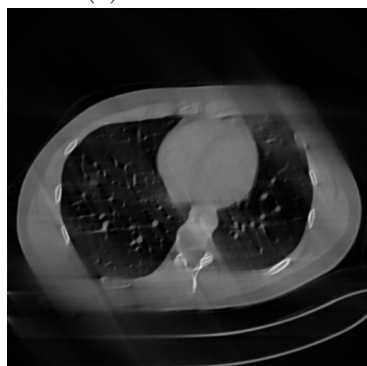
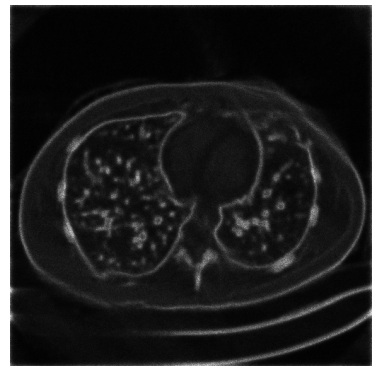
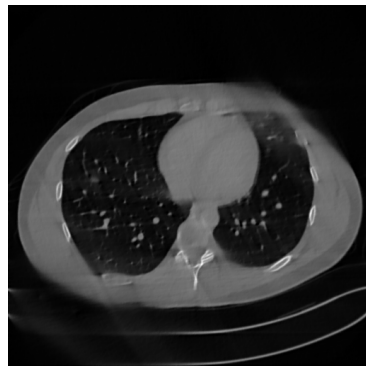
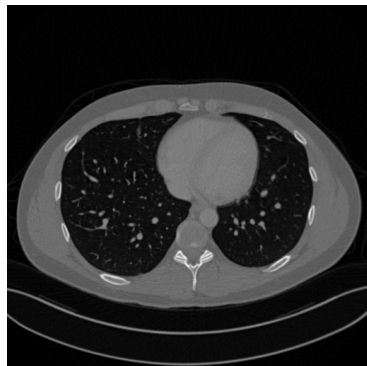


Figure 3: CT reconstruction results. DC-LA mean achieves SSIM 0.8493 and PSNR 26.2109. PSM MAP with iterations: 2k (SSIM 0.7586, PSNR 24.2803), 10k (SSIM 0.8488, PSNR 26.2498), 20k (SSIM 0.8501, PSNR 26.5246).

Luigi Ambrosio, Nicola Gigli, and Giuseppe Savaré. *Gradient flows: in metric spaces and in the space of probability measures*. Springer, 2005.

Le Thi Hoai An and Pham Dinh Tao. The DC (difference of convex functions) programming and DCA revisited with DC models of real world nonconvex optimization problems. *Annals of operations research*, 133(1):23–46, 2005.

Heinz H Bauschke and Patrick L Combettes. Correction to: convex analysis and monotone operator theory in hilbert spaces. In *Convex analysis and monotone operator theory in Hilbert spaces*. Springer, 2020.

Emmanuel J Candes, Michael B Wakin, and Stephen P Boyd. Enhancing sparsity by reweighted 11 minimization. *Journal of Fourier analysis and applications*, 14(5):877–905, 2008.

Sinho Chewi. Log-concave sampling. *Book draft available at <https://chewisinho.github.io>*, 9: 17–18, 2023.

Tiangang Cui, Sergey Dolgov, and Olivier Zahm. Scalable conditional deep inverse Rosenblatt transports using tensor trains and gradient-based dimension reduction. *Journal of Computational Physics*, 485:112103, 2023.

Ying Cui, Jong-Shi Pang, and Bodhisattva Sen. Composite difference-max programs for modern statistical estimation problems. *SIAM Journal on Optimization*, 28(4):3344–3374, 2018.

Valentin De Bortoli and Alain Durmus. Convergence of diffusions and their discretizations: from continuous to discrete processes and back. *arXiv preprint arXiv:1904.09808*, 2019.

Arnaud Debussche, Ying Hu, and Gianmario Tessitore. Ergodic BSDEs under weak dissipative assumptions. *Stochastic Processes and their applications*, 121(3):407–426, 2011.

Michael Ziyang Diao, Krishna Balasubramanian, Sinho Chewi, and Adil Salim. Forward-backward Gaussian variational inference via JKO in the Bures-Wasserstein space. In *International Conference on Machine Learning*, pages 7960–7991. PMLR, 2023.

Alain Durmus, Szymon Majewski, and Błażej Miasojedow. Analysis of Langevin Monte Carlo via convex optimization. *The Journal of Machine Learning Research*, 20(1):2666–2711, 2019.

Weinan E, Weiqing Ren, and Eric Vanden-Eijnden. String method for the study of rare events. *Phys. Rev. B*, 66:052301, Aug 2002. doi:[10.1103/PhysRevB.66.052301](https://doi.org/10.1103/PhysRevB.66.052301). URL <https://link.aps.org/doi/10.1103/PhysRevB.66.052301>.

Andreas Eberle. Reflection couplings and contraction rates for diffusions. *Probability theory and related fields*, 166(3):851–886, 2016.

Andreas Eberle and Mateusz B. Majka. Quantitative contraction rates for Markov chains on general state spaces. *Electronic Journal of Probability*, 24:1–36, 2019.

Matthias J Ehrhardt, Lorenz Kuger, and Carola-Bibiane Schönlieb. Proximal Langevin sampling with inexact proximal mapping. *SIAM Journal on Imaging Sciences*, 17(3):1729–1760, 2024.

Jianqing Fan and Runze Li. Variable selection via nonconcave penalized likelihood and its oracle properties. *Journal of the American statistical Association*, 96(456):1348–1360, 2001.

Grégoire Ferré and Gabriel Stoltz. Error estimates on ergodic properties of discretized Feynman–Kac semigroups. *Numerische Mathematik*, 143(2):261–313, 2019.

Donald Geman and Chengda Yang. Nonlinear image recovery with half-quadratic regularization. *IEEE transactions on Image Processing*, 4(7):932–946, 1995.

Stuart Geman and Donald Geman. Stochastic relaxation, gibbs distributions, and the Bayesian restoration of images. *IEEE Transactions on pattern analysis and machine intelligence*, PAMI-6(6):721–741, 1984.

J-B Hiriart-Urruty. More on second-order properties of the Moreau regularization-approximation of a convex function. *Optimization Methods and Software*, 39(3):519–533, 2024.

Jean-Baptiste Hiriart-Urruty and Claude Lemaréchal. *Fundamentals of convex analysis*. Springer Science & Business Media, 2004.

Quanqi Hu, Qi Qi, Zhaosong Lu, and Tianbao Yang. Single-loop stochastic algorithms for difference of max-structured weakly convex functions. *Advances in Neural Information Processing Systems*, 37:56738–56765, 2024.

Tim Johnston, Iosif Lytras, Nikolaos Makras, and Sotirios Sabanis. The performance of the unadjusted langevin algorithm without smoothness assumptions. *Transactions on Machine Learning Research (TMLR)*, 2025.

Jinyoung Jun, Lei Chu, Jiahao Li, Yan Lu, and Chang-Su Kim. Perfecting depth: Uncertainty-aware enhancement of metric depth. *arXiv preprint arXiv:2506.04612*, 2025.

Hoai An Le Thi, T Pham Dinh, Hoai Minh Le, and Xuan Thanh Vo. DC approximation approaches for sparse optimization. *European Journal of Operational Research*, 244(1):26–46, 2015.

Hoai An Le Thi, Van Ngai Huynh, Tao Pham Dinh, and Hoang Phuc Hau Luu. Stochastic difference-of-convex-functions algorithms for nonconvex programming. *SIAM Journal on Optimization*, 32(3):2263–2293, 2022.

Tianxiang Liu and Ting Kei Pong. Further properties of the forward–backward envelope with applications to difference-of-convex programming. *Computational Optimization and Applications*, 67(3):489–520, 2017.

Yifei Lou and Ming Yan. Fast L1–L2 minimization via a proximal operator. *Journal of Scientific Computing*, 74(2):767–785, 2018.

Sebastian Lunz, Ozan Öktem, and Carola-Bibiane Schönlieb. Adversarial regularizers in inverse problems. *Advances in neural information processing systems*, 31, 2018.

Ziyan Luo, Yingnan Wang, and Xianglilan Zhang. New improved penalty methods for sparse reconstruction based on difference of two norms. Technical report, Technical report, 2013. doi: 10.13140/RG. 2.1. 3256.3369, 2015.

Hoang Phuc Hau Luu, Hanlin Yu, Bernardo Williams, Petrus Mikkola, Marcelo Hartmann, Kai Puolamäki, and Arto Klami. Non-geodesically-convex optimization in the Wasserstein space. *Advances in Neural Information Processing Systems*, 37:16772–16809, 2024.

Hoang Phuc Hau Luu, Hanlin Yu, Bernardo Williams, Marcelo Hartmann, and Arto Klami. Stochastic variance-reduced Gaussian variational inference on the Bures-Wasserstein manifold. *Proceedings of the Thirteenth International Conference on Learning Representations (ICLR)*, 2025.

Tung Duy Luu, Jalal Fadili, and Christophe Chesneau. Sampling from non-smooth distributions through Langevin diffusion. *Methodology and Computing in Applied Probability*, 23(4):1173–1201, 2021.

Taylor R Moen, Baiyu Chen, David R Holmes III, Xinhui Duan, Zhicong Yu, Lifeng Yu, Shuai Leng, Joel G Fletcher, and Cynthia H McCollough. Low-dose CT image and projection dataset. *Medical physics*, 48(2):902–911, 2021.

Petr Mokrov, Alexander Korotin, Lingxiao Li, Aude Genevay, Justin M Solomon, and Evgeny Burnaev. Large-scale Wasserstein gradient flows. *Advances in Neural Information Processing Systems*, 34:15243–15256, 2021.

Wenlong Mou, Nicolas Flammarion, Martin J Wainwright, and Peter L Bartlett. Improved bounds for discretization of Langevin diffusions: Near-optimal rates without convexity. *Bernoulli*, 28(3):1577–1601, 2022.

Maher Nouiehed, Jong-Shi Pang, and Meisam Razaviyayn. On the pervasiveness of difference-convexity in optimization and statistics. *Mathematical Programming*, 174(1):195–222, 2019.

Tao Pham Dinh and Hoai An Le Thi. Convex analysis approach to DC programming: theory, algorithms and applications. *Acta mathematica vietnamica*, 22(1):289–355, 1997.

Miklós Rásonyi and Kinga Tikosi. On the stability of the stochastic gradient Langevin algorithm with dependent data stream. *Statistics & Probability Letters*, 182:109321, 2022.

Marien Renaud, Jiaming Liu, Valentin De Bortoli, Andrés Almansa, and Ulugbek S Kamilov. Plug-and-play posterior sampling under mismatched measurement and prior models. In *Proceedings of the Twelfth International Conference on Learning Representations (ICLR)*, 2023.

Marien Renaud, Valentin De Bortoli, Arthur Leclaire, and Nicolas Papadakis. From stability of Langevin diffusion to convergence of proximal MCMC for non-log-concave sampling. *Advances in Neural Information Processing Systems*, 2025a.

Marien Renaud, Arthur Leclaire, and Nicolas Papadakis. On the Moreau envelope properties of weakly convex functions. *arXiv preprint arXiv:2509.13960*, 2025b.

Gareth O Roberts and Richard L Tweedie. Exponential convergence of langevin distributions and their discrete approximations. *Bernoulli*, 1996.

Olaf Ronneberger, Philipp Fischer, and Thomas Brox. U-net: Convolutional networks for biomedical image segmentation. In *International Conference on Medical image computing and computer-assisted intervention*, pages 234–241. Springer, 2015.

Adil Salim and Peter Richtarik. Primal dual interpretation of the proximal stochastic gradient Langevin algorithm. *Advances in Neural Information Processing Systems*, 33:3786–3796, 2020.

Adil Salim, Dmitry Kovalev, and Peter Richtárik. Stochastic proximal Langevin algorithm: Potential splitting and nonasymptotic rates. *Advances in Neural Information Processing Systems*, 32, 2019.

Adil Salim, Anna Korba, and Giulia Luise. The Wasserstein proximal gradient algorithm. *Advances in Neural Information Processing Systems*, 33:12356–12366, 2020.

Daniel Sanz-Alonso, Andrew Stuart, and Armeen Taeb. *Inverse Problems and Data Assimilation*. London Mathematical Society Student Texts. Cambridge University Press, 2023.

D Andersen Sorensen, S Andersen, D Gianola, and I Korsgaard. Bayesian inference in threshold models using Gibbs sampling. *Genetics Selection Evolution*, 27(3):229–249, 1995.

Kaizhao Sun and Xu Andy Sun. Algorithms for difference-of-convex programs based on difference-of-moreau-envelopes smoothing. *INFORMS Journal on Optimization*, 5(4):321–339, 2023.

Yu Sun, Zihui Wu, Yifan Chen, Berthy T Feng, and Katherine L Bouman. Provable probabilistic imaging using score-based generative priors. *IEEE Transactions on Computational Imaging*, 2024.

Joshua Trzasko and Armando Manduca. Highly undersampled magnetic resonance image reconstruction via homotopic l_0 -minimization. *IEEE Transactions on Medical Imaging*, 28(1):106–121, 2008.

Cédric Villani et al. *Optimal transport: old and new*, volume 338. Springer, 2008.

Zhongjian Wang, Jack Xin, and Zhiwen Zhang. Sharp error estimates on a stochastic structure-preserving scheme in computing effective diffusivity of 3D chaotic flows. *Multiscale Modeling & Simulation*, 19(3):1167–1189, 2021.

Quanming Yao and James T Kwok. Efficient learning with a family of nonconvex regularizers by redistributing nonconvexity. *Journal of Machine Learning Research*, 18(179):1–52, 2018.

Penghang Yin, Yifei Lou, Qi He, and Jack Xin. Minimization of l_1 - l_2 for compressed sensing. *SIAM Journal on Scientific Computing*, 37(1):A536–A563, 2015.

Cun-Hui Zhang. Nearly unbiased variable selection under minimax concave penalty. *The Annals of Statistics*, 38(2):894–942, 2010a.

Tong Zhang. Analysis of multi-stage convex relaxation for sparse regularization. *Journal of Machine Learning Research*, 11(3), 2010b.

Yasi Zhang and Oscar Leong. Learning difference-of-convex regularizers for inverse problems: A flexible framework with theoretical guarantees. *arXiv preprint arXiv:2502.00240*, 2025.

A Sub-Gaussian tails

Let V satisfy Assumptions 1 and 2, we show that $\pi \propto e^{-V}$ has sub-Gaussian tails. Let $g_1(x) \in \partial r_1(x)$ and $g_2(x) \in \partial r_2(x)$ be some measurable selections and let $g(x) := \nabla f(x) + g_1(x) - g_2(x)$, under Assumption 2: there exist $R_0 \geq 0$, $\mu > 0$ such that

$$\langle g(x) - g(y), x - y \rangle \geq \mu \|x - y\|^2$$

for all $\|x - y\| \geq R_0$. Now fix x such that $\|x\| > R_0$, we have

$$\langle g(tx) - g(0), x \rangle \geq \mu t \|x\|^2$$

whenever $t \geq R_0/\|x\|$. Let $t_0 := R_0/\|x\| < 1$, by applying Mean Value Theorem (MVT) to f, r_1, r_2 (see [Hiriart-Urruty and Lemaréchal, 2004, Theorem 2.3.4] for MTV for convex functions), we get

$$\begin{aligned} V(x) - V(0) &= \int_0^1 \langle g(tx), x \rangle dt \\ &= \int_0^{t_0} \langle g(tx), x \rangle dt + \int_{t_0}^1 \langle g(tx), x \rangle dt \\ &\geq \int_0^{t_0} \langle g(tx), x \rangle dt + \int_{t_0}^1 (\mu t \|x\|^2 + \langle g(0), x \rangle) dt \\ &= \int_0^{t_0} \langle g(tx), x \rangle dt + \frac{\mu}{2}(1 - t_0^2) \|x\|^2 + (1 - t_0) \langle g(0), x \rangle \\ &\geq \int_0^{t_0} \langle g(tx), x \rangle dt + \frac{\mu}{2} \|x\|^2 - \frac{\mu}{2} R_0^2 - \|g(0)\| \|x\|. \end{aligned}$$

On the other hand, $\|g(tx)\|$ is bounded for all $t \in [0, t_0]$. Indeed, since f is L_f -smooth,

$$\|\nabla f(tx)\| \leq L_f t \|x\| + \|\nabla f(0)\| \leq L_f R_0 + \|\nabla f(0)\|.$$

Using the convexity of each r_i ,

$$r_i(y) - r_i(tx) \geq \langle g_i(tx), y - tx \rangle, \quad \forall y \in \mathbb{R}^d.$$

A convex function is locally Lipschitz, therefore, there exists $M_i > 0$ such that

$$|r_i(u) - r_i(v)| \leq M_i \|u - v\|, \quad \forall u, v \in B'(0, R_0 + 1)$$

where $B'(0, R_0 + 1)$ denotes the closed ball with radius $R_0 + 1$.

Now let $\epsilon > 0$ such that $\epsilon \|g_i(tx)\| \leq 1$ and let $y = tx + \epsilon g_i(tx)$, it holds $y \in B'(0, R_0 + 1)$. Therefore,

$$\langle g_i(tx), \epsilon g_i(tx) \rangle \leq M_i \epsilon \|g_i(tx)\| \tag{17}$$

implying $\|g_i(tx)\| \leq M_i$ for all $t \in [0, t_0]$.

Therefore, there exists $C, D > 0$ such that

$$V(x) - V(0) \geq \frac{\mu}{2} \|x\|^2 - C \|x\| - \frac{\mu}{2} R_0^2 \geq \frac{\mu}{4} \|x\|^2 - D,$$

implying that π has sub-Gaussian tails. This further implies π^λ (8) and $\pi^{\lambda, \gamma}$ (14) have sub-Gaussian tails. Indeed, it holds $V_\lambda(x) \geq V(x) - (\lambda G_1^2)/2$ for all x . On the other hand, $\nabla(r_1^\lambda)^\gamma(x) = \nabla r_1^\lambda(\text{Prox}_{\gamma r_1^\lambda}(x)) \in \partial r_1(\text{Prox}_{\lambda r_1}(\text{Prox}_{\gamma r_1^\lambda}(x)))$, hence, $\|\nabla(r_1^\lambda)^\gamma(x)\| \leq G_1$ for all x . Therefore

$$f(x) + (r_1^\lambda)^\gamma(x) - r_2^\lambda(x) \geq f(x) + r_1^\lambda(x) - r_2^\lambda(x) - \frac{\gamma G_1^2}{2}. \tag{18}$$

B Finite moments of random variables

We first show that: if X_0 has finite p' moment ($p' \geq 1$), $\{X_k\}, \{Y_k\}$ generated by DC-LA have finite p' -th moment.

By induction, suppose that $\mathbb{E}\|X_k\|^{p'} < +\infty$, we show $\mathbb{E}\|Y_{k+1}\|^{p'} < +\infty$ and $\mathbb{E}\|X_{k+1}\|^{p'} < +\infty$. Indeed, by applying Minkowski inequality,

$$\begin{aligned} (\mathbb{E}\|Y_{k+1}\|^{p'})^{\frac{1}{p'}} &\leq (\mathbb{E}\|X_k\|^{p'})^{\frac{1}{p'}} + \gamma(\mathbb{E}\|\nabla f(X_k)\|^{p'})^{\frac{1}{p'}} + \gamma(\mathbb{E}\|\nabla r_2^\lambda(X_k)\|^{p'})^{\frac{1}{p'}} + \sqrt{2\gamma}(\mathbb{E}\|Z_{k+1}\|^{p'})^{\frac{1}{p'}} \\ &\leq (\mathbb{E}\|X_k\|^{p'})^{\frac{1}{p'}} + \gamma(\|\nabla f(0)\| + L_f(\mathbb{E}\|X_k\|^{p'})^{\frac{1}{p'}}) \\ &\quad + \gamma \left(\|\nabla r_2^\lambda(0)\| + \frac{1}{\lambda}(\mathbb{E}\|X_k\|^{p'})^{\frac{1}{p'}} \right) + \sqrt{2\gamma}(\mathbb{E}\|Z_{k+1}\|^{p'})^{\frac{1}{p'}} < +\infty. \end{aligned}$$

Then, using the non-expansiveness of the proximal operator,

$$(\mathbb{E}\|X_{k+1}\|^{p'})^{\frac{1}{p'}} = (\mathbb{E}\|\text{Prox}_{\gamma r_1^\lambda}(Y_{k+1})\|^{p'})^{\frac{1}{p'}} \leq \|\text{Prox}_{\gamma r_1^\lambda}(0)\| + (\mathbb{E}\|Y_{k+1}\|^{p'})^{\frac{1}{p'}} < +\infty.$$

Similarly, $\mathbb{E}\|\bar{Y}_k\|^{p'} < +\infty$ where $\{\bar{Y}_k\}$ is defined in (13) if $\mathbb{E}\|\bar{Y}_1\|^{p'} < +\infty$.

C Unrolled DC-LA

The unrolled form of DC-LA is

$$\begin{aligned} X_{k+1} &= X_k - \frac{\gamma\lambda}{\gamma+\lambda} \nabla f(X_k) - \frac{\gamma}{\gamma+\lambda} \text{Prox}_{\lambda r_2}(X_k) + \frac{\lambda\sqrt{2\gamma}}{\gamma+\lambda} Z_{k+1} \\ &\quad + \frac{\gamma}{\gamma+\lambda} \text{Prox}_{(\lambda+\gamma)r_1} \left(\frac{\lambda+\gamma}{\lambda} X_k - \gamma \nabla f(X_k) - \frac{\gamma}{\lambda} \text{Prox}_{\lambda r_2}(X_k) + \sqrt{2\gamma} Z_{k+1} \right). \end{aligned}$$

D DC regularizers

We first recall some non-convex regularizers and their DC decompositions. We then show that the first DC component of each regularizer is Lipschitz continuous, while the second is either Lipschitz continuous, or is differentiable with Hölder or Lipschitz continuous gradient. Hence, Theorems 8 and 9 can be invoked accordingly, provided the distant dissipative assumptions are satisfied.

D.1 DC regularizers with two nonsmooth components

(1) $\ell_1 - \ell_2$ regularizer [Yin et al., 2015, Lou and Yan, 2018]

$$r(x) = \|x\|_1 - \|x\|_2.$$

(2) $\ell_1 - \ell_{\sigma_q}$ regularizer [Luo et al., 2015] We define $\|x\|_{\sigma_q} = \sum_{i=1}^q |x_{[i]}|$ where $x_{[i]}$ represents the i -th element of x ordered by magnitude. Let

$$r(x) = \|x\|_1 - \|x\|_{\sigma_q}.$$

(3) Capped ℓ_1 [Zhang, 2010b, Le Thi et al., 2015] Let $\theta > 0$ be a parameter. We define

$$r(x) = \sum_{i=1}^d \min\{1, \theta|x_i|\} = \theta\|x\|_1 - \sum_{i=1}^d (\theta|x_i| - \min\{1, \theta|x_i|\}).$$

(4) **PiL [Le Thi et al., 2015]** Let $\theta > 0, a > 1$ be parameters, we define

$$\begin{aligned} r(x) &= \sum_{i=1}^d \min \left\{ 1, \max \left\{ 0, \frac{\theta|x_i| - 1}{a-1} \right\} \right\} \\ &= \frac{\theta}{a-1} \sum_{i=1}^d \max \left\{ \frac{1}{\theta}, |x_i| \right\} - \sum_{i=1}^d \left(\frac{\theta}{a-1} \max \left\{ \frac{1}{\theta}, |x_i| \right\} - \min \left\{ 1, \max \left\{ 0, \frac{\theta|x_i| - 1}{a-1} \right\} \right\} \right). \end{aligned}$$

(5) $\ell_1 - \ell_2^p$ regularizer ($1 < p < 2$)

$$r(x) = \|x\|_1 - \|x\|_2^p.$$

The regularizers (1), (2), (3), (4) have both non-differentiable DC components, while the regularizer (5) has non-differentiable r_1 and differentiable r_2 whose gradient is Hölder continuous.

Since ℓ_1 is \sqrt{d} -Lipschitz continuous (d is the dimension), the first DC components of $\ell_1 - \ell_2$, $\ell_1 - \ell_{\sigma_q}$, $\ell_1 - \ell_2^p$ are \sqrt{d} -Lipschitz continuous and that of Capped ℓ_1 is $\theta\sqrt{d}$ -Lipschitz continuous. Regarding the first DC component of PiL, it is straightforward to verify that

$$\left| \max \left\{ \frac{1}{\theta}, |u| \right\} - \max \left\{ \frac{1}{\theta}, |v| \right\} \right| \leq |u - v|, \quad \forall u, v \in \mathbb{R}.$$

Therefore, the first DC component of PiL is $\frac{\theta}{a-1}\sqrt{d}$ -Lipschitz continuous.

Now the second DC component of the $\ell_1 - \ell_2$ regularizer is 1-Lipschitz continuous, while the second DC component of the $\ell_1 - \ell_{\sigma_q}$ regularizer is \sqrt{d} -Lipschitz continuous. The latter is due to

$$|\|x\|_{\sigma_q} - \|y\|_{\sigma_q}| \leq \|x - y\|_{\sigma_q} \leq \|x - y\|_1 \leq \sqrt{d}\|x - y\|_2.$$

It is direct to verify that $|\min\{1, \theta|u|\} - \min\{1, \theta|v|\}| \leq \theta|u - v|$, therefore the second DC component of Capped ℓ_1 is $2\theta\sqrt{d}$ -Lipschitz continuous. We then have

$$\begin{aligned} &\left| \min \left\{ 1, \max \left\{ 0, \frac{\theta|u| - 1}{a-1} \right\} \right\} - \min \left\{ 1, \max \left\{ 0, \frac{\theta|v| - 1}{a-1} \right\} \right\} \right| \\ &\leq \left| \max \left\{ 0, \frac{\theta|u| - 1}{a-1} \right\} - \max \left\{ 0, \frac{\theta|v| - 1}{a-1} \right\} \right| \\ &\leq \frac{\theta}{a-1}|u - v|. \end{aligned}$$

Therefore, the second component of PiL is $2\frac{\theta}{a-1}\sqrt{d}$ -Lipschitz continuous.

Lastly, $r_2(x) := \|x\|^p$ has $(p-1, C)$ -Hölder continuous gradient for some $C > 0$. Indeed, the gradient is given by $\|x\|^{p-2}x$ if $x \neq 0$ and 0 if $x = 0$. Indeed, as a standard result, there exists $C > 0$ such that

$$|\|x\|^{p-2}x - \|y\|^{p-2}y| \leq C\|x - y\|^{p-1}, \quad \forall x, y \neq 0.$$

For completeness, we give a proof. We consider two cases: (a) $\|x - y\| \geq \frac{1}{2} \max\{\|x\|, \|y\|\}$ and (b) $\|x - y\| < \frac{1}{2} \max\{\|x\|, \|y\|\}$.

Under case (a),

$$|\|x\|^{p-2}x - \|y\|^{p-2}y| \leq \|x\|^{p-1} + \|y\|^{p-1} \leq 2^p\|x - y\|^{p-1}.$$

Under case (b), without loss of generality, assume that $\|x\| \geq \|y\|$. Note that $[x, y]$ cannot contain the origin. Applying Mean Value Theorem, there exists $z \in [x, y]$:

$$\begin{aligned} |\|x\|^{p-2}x - \|y\|^{p-2}y| &\leq \|\nabla^2 r_2(z)\| \|x - y\| \\ &= \left\| p\|z\|^{p-2}I + p(p-2)\|z\|^{p-4}zz^\top \right\| \|x - y\| \\ &\leq C'\|z\|^{p-2}\|x - y\|. \end{aligned}$$

On the other hand

$$\|z\| \geq \|x\| - \|x - z\| \geq \|x\| - \|x - y\| > \frac{1}{2}\|x\|.$$

Therefore,

$$\|z\|^{p-2}\|x - y\| \leq C''\|x\|^{p-2}\|x - y\| \leq C\|x - y\|^{p-1}.$$

D.2 DC regularizers with nonsmooth first DC component and smooth second DC component

[Yao and Kwok \[2018\]](#) identified a family of DC regularizers whose first component is nonsmooth and second is smooth. This family of regularizers can be written as

$$r(x) = \sum_{i=1}^K \mu_i \kappa(\|A_i x\|_2)$$

where $\mu_i \geq 0$ for all $i = \overline{1, K}$ and A_i are matrices (to induce structured sparsity like group LASSO, fused LASSO or graphical LASSO [\[Yao and Kwok, 2018\]](#)), $\kappa : [0, \infty) \rightarrow [0, \infty)$ such that κ is concave, non-decreasing, ρ -smooth for some $\rho > 0$ with κ' non-differentiable at finite many points, $\kappa(0) = 0$. As shown in Table 1 in [\[Yao and Kwok, 2018\]](#), this structure covers German penalty (GP), log-sum penalty (LSP), Laplace, Minimax Concave Penalty (MCP), and Smoothly Clipped Absolute Deviation (SCAD).

Let $\kappa_0 := \kappa'(0)$, r has the following DC decomposition

$$r(x) = \kappa_0 \sum_{i=1}^K \mu_i \|A_i x\|_2 - \sum_{i=1}^K (\kappa_0 \mu_i \|A_i x\|_2 - \mu_i \kappa(\|A_i x\|_2)).$$

The first DC component of r is nonsmooth, while the second can be shown to be smooth [\[Yao and Kwok, 2018\]](#). We further see that

$$|\|A_i x\|_2 - \|A_i y\|_2| \leq \|A_i x - A_i y\|_2 \leq \|A_i\|_F \|x - y\|_2$$

where $\|A_i\|_F$ is the Frobenius norm of A_i . Therefore the first DC component of r is $\kappa_0(\sum \mu_i \|A_i\|_F)$ -Lipschitz continuous.

E On Assumption 3 in [\[Renaud et al., 2025a\]](#)

Let $\rho > 0$, suppose that r is ρ -weakly convex, i.e., $r + \frac{\rho}{2}\|\cdot\|^2$ is convex.

We recall Assumption 3 in [\[Renaud et al., 2025a\]](#) as follows.

Assumption. (i) $\forall \gamma \in (0, \frac{1}{\rho})$, r is L_r -smooth on $\text{Prox}_{\gamma r}(\mathbb{R}^d)$.

(ii) r^γ is μ -strongly convex at infinity with $\mu \geq 8L_f + 4L_r$, i.e, there exists $\gamma_1 > 0$ and $R_0 \geq 0$ such that $\forall \gamma \in (0, \gamma_1]$, $\nabla^2 r^\gamma \succeq \mu I$ on $\mathbb{R}^d \setminus B(0, R_0)$.

We show that this assumption does not hold. Let $\gamma \in (0, \frac{1}{\rho})$. For $x \in \mathbb{R}^d$, recall that

$$\text{Prox}_{\gamma r}(x) = \operatorname{argmin}_y \left\{ r(y) + \frac{1}{2\gamma} \|y - x\|^2 \right\}.$$

By the first-order optimality condition

$$0 \in \partial \left(r + \frac{1}{2\gamma} \|\cdot - x\|^2 \right) (\text{Prox}_{\gamma r}(x)). \quad (19)$$

By Assumption (i), r is differentiable at $\text{Prox}_{\gamma r}(x)$, (19) becomes

$$0 = \nabla r(\text{Prox}_{\gamma r}(x)) + \frac{1}{\gamma}(\text{Prox}_{\gamma r}(x) - x)$$

On the other hand, since $\gamma\rho < 1$, it follows from [Renaud et al., 2025a, Lemma 12],

$$\nabla r^\gamma(x) = \frac{1}{\gamma}(x - \text{Prox}_{\gamma r}(x))$$

so $\nabla r^\gamma(x) = \nabla r(\text{Prox}_{\gamma r}(x))$ for all x . Now that

$$\begin{aligned} \|\nabla r^\gamma(x) - \nabla r^\gamma(y)\| &= \|\nabla r(\text{Prox}_{\gamma r}(x)) - \nabla r(\text{Prox}_{\gamma r}(y))\| \\ &\leq L_r \|\text{Prox}_{\gamma r}(x) - \text{Prox}_{\gamma r}(y)\| \leq \frac{L_r}{1 - \gamma\rho} \|x - y\| \end{aligned}$$

since $\text{Prox}_{\gamma r}$ is $\frac{1}{1 - \gamma\rho}$ -Lipschitz [Renaud et al., 2025b, Lemma 11]. Therefore r^γ is $\frac{L_r}{1 - \gamma\rho}$ -smooth in \mathbb{R}^d .

From Assumption (ii), let x, y be two points far away from the origin so that the segment $[x, y]$ does not intersect $B(0, R_0)$. Let $\gamma < \min\{\frac{3}{4\rho}, \gamma_1\}$,

$$\nabla r^\gamma(x) - \nabla r^\gamma(y) = \int_0^1 \nabla^2 r^\gamma(tx + (1-t)y)(x - y) dt.$$

Therefore

$$\langle x - y, \nabla r^\gamma(x) - \nabla r^\gamma(y) \rangle = \int_0^1 (x - y)^\top \nabla^2 r^\gamma(tx + (1-t)y)(x - y) dt \geq \mu \|x - y\|^2$$

On the other hand,

$$\langle x - y, \nabla r^\gamma(x) - \nabla r^\gamma(y) \rangle \leq \|x - y\| \|\nabla r^\gamma(x) - \nabla r^\gamma(y)\| \leq \frac{L_r}{1 - \gamma\rho} \|x - y\|^2.$$

These inequalities imply $\mu \leq \frac{L_r}{1 - \gamma\rho}$. Therefore, the condition $\mu \geq 4L_r + 8L_f$ implies $\gamma \geq \frac{3}{4\rho}$ and this is a contradiction.

F Non-weakly-convex DC regularizers

We show the following DC regularizers are not weakly convex.

F.1 $\ell_1 - \ell_2$

Let $r(x) = \|x\|_1 - \|x\|_2$. Suppose that there exists $\alpha > 0$ such that $u(x) := r(x) + \alpha\|x\|_2^2$ is convex.

Let's pick x^* with positive entries such that $\|x^*\|_2 < \frac{1}{2\alpha}$. We have $\nabla^2 \|\cdot\|_1(x^*) = 0$ and

$$\nabla^2 \|\cdot\|_2(x^*) = \frac{1}{\|x^*\|_2} I - \frac{1}{\|x^*\|_2^3} x^* x^{*\top}.$$

Therefore,

$$\nabla^2 u(x^*) = 2\alpha I - \frac{1}{\|x^*\|_2} I + \frac{1}{\|x^*\|_2^3} x^* x^{*\top}.$$

Let $d \in \mathbb{R}^d, \|d\|_2 = 1$ such that d is orthogonal to x^* , it follows that

$$d^\top \nabla^2 u(x^*) d = 2\alpha - \frac{1}{\|x^*\|_2} < 0.$$

So u is not convex. This is a contradiction, we conclude that r is not weakly convex.

F.2 $\ell_1 - \ell_{\sigma_q}$

We define $\|x\|_{\sigma_q} = \sum_{i=1}^q |x_{[i]}|$ where $x_{[i]}$ represents the i -th element of x ordered by magnitude. Note that when $q = 1$, $\|x\|_{\sigma_q} = \|x\|_\infty$.

Now let $r(x) = \|x\|_1 - \|x\|_{\sigma_q}$ and suppose that there exists $\alpha > 0$ such that $u(x) = r(x) + \alpha\|x\|_2^2$ is convex.

Let $A > 1$ and let x such that

$$x_1 = x_2 = \dots = x_{q-1} = A, |x_q| < 1, |x_{q+1}| < 1, x_{q+2} = \dots = x_d = 0.$$

Hence $\|x\|_{\sigma_q} = (q-1)A + \max\{|x_q|, |x_{q+1}|\}$. Therefore

$$r(x) = |x_q| + |x_{q+1}| - \max\{|x_q|, |x_{q+1}|\} = \min\{|x_q|, |x_{q+1}|\}.$$

Consider the 2D slice, the function $\bar{u}(x_q, x_{q+1}) = \min\{|x_q|, |x_{q+1}|\} + \alpha(x_q^2 + x_{q+1}^2)$ is convex in $(-1, 1) \times (-1, 1)$. Let $0 < \epsilon < 1$,

$$\bar{u}(\epsilon, 0) + \bar{u}(0, \epsilon) \geq 2\bar{u}\left(\frac{\epsilon}{2}, \frac{\epsilon}{2}\right)$$

reducing to

$$2\alpha\epsilon^2 \geq 2\left(\frac{\epsilon}{2} + \alpha\frac{\epsilon^2}{2}\right) \Rightarrow \alpha\epsilon \geq 1,$$

which cannot hold for small ϵ . We get a contradiction.

F.3 Capped- ℓ_1

Let $\theta > 0$, we define

$$r(x) = \sum_{i=1}^d \min\{1, \theta|x_i|\}.$$

Since $\text{Cap}\ell_1$ is separable, we only need to show it is not weakly convex in 1D.

Now in 1D, by contradiction, suppose there is $\alpha > 0$ such that $u(x) = r(x) + \alpha x^2$ is convex.

Let $\epsilon \in (0, \frac{1}{2\theta})$ and we denote $x^+ = \frac{1}{\theta} + \epsilon$, $x^- = \frac{1}{\theta} - \epsilon > 0$. Mid-point inequality reads

$$2u\left(\frac{1}{2}(x^+ + x^-)\right) \leq u(x^+) + u(x^-)$$

or

$$2\left(1 + \alpha\frac{1}{\theta^2}\right) \leq 1 + \alpha\left(\frac{1}{\theta} + \epsilon\right)^2 + (1 - \theta\epsilon) + \alpha\left(\frac{1}{\theta} - \epsilon\right)^2.$$

which reduces to $2\alpha\epsilon \geq \theta$. This cannot hold for small ϵ and is a contradiction.

F.4 DICNNs with leaky ReLU activations

Let r be given by $r(x) = r_1(x) - r_2(x)$ where r_1 and r_2 are two ICNNs with leaky ReLU activations. r_1 and r_2 are then two convex, piecewise linear functions with respect to x . In general, r is not weakly convex. To see this, take a 1D slice, $-r_2$ restricted to this slice is a 1D piecewise concave function that is not a linear function in general. If r_1 restricted to the same slice cannot exactly cancel out the concavity of $-r_2$, no amount of quadratic $\alpha\|x\|^2$ can.

G Example on discontinuous proximal operator of a DC function

Consider the following 1D example, $r(x) = -|x|$. Let $\gamma > 0$ and let $|v| < \gamma$, we consider

$$\text{Prox}_{\gamma r}(v) = \operatorname{argmin}_x \left\{ \frac{1}{2\gamma}(x - v)^2 - |x| \right\}$$

Let $u(x) = \frac{1}{2}(x - v)^2 - \gamma|x|$. For $x > 0$, u is minimized at $x^+ = v + \gamma > 0$; For $x < 0$, u is minimized at $x^- = v - \gamma$. Comparing $f(x^+)$, $f(x^-)$ and $f(0)$ we conclude: if $v = 0$, both x^+, x^- minimize u , if $v > 0$, x^+ is the unique minimizer, and if $v < 0$, x^- is the unique minimizer. Therefore,

$$\text{Prox}_{\gamma r}(v) = \begin{cases} v + \gamma & \text{if } v > 0 \\ \{v, -v\} & \text{if } v = 0, \\ v - \gamma & \text{if } v < 0. \end{cases}$$

Hence, $\text{Prox}_{\gamma r}$ is multivalued and discontinuous at 0, as reflected in Figure 4.

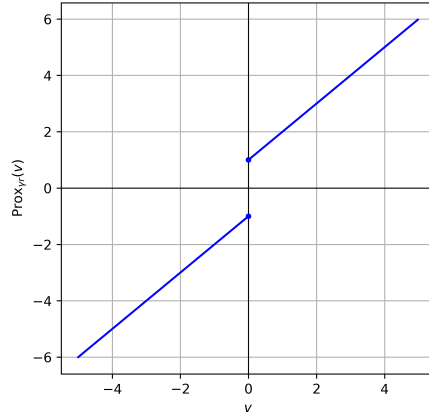


Figure 4: Plot of $\text{Prox}_{-|.|}$

H Lemmas

Lemma 10. *Let g be a convex function and $\lambda, \gamma > 0$, it holds*

$$\text{Prox}_{\gamma g^\lambda}(x) = \frac{1}{\gamma + \lambda} \left(\gamma \text{Prox}_{(\gamma + \lambda)g}(x) + \lambda x \right).$$

Proof. This is a standard and known result. For completeness, we give a proof as follows. $\text{Prox}_{\gamma g^\lambda}(x)$ is the solution of

$$\min_y \left\{ g^\lambda(y) + \frac{1}{2\gamma} \|x - y\|^2 \right\} \tag{20}$$

By using the definition of Moreau envelope, the problem (20) can be cast to

$$\min_{(y,z)} \left\{ g(z) + \frac{1}{2\lambda} \|y - z\|^2 + \frac{1}{2\gamma} \|x - y\|^2 \right\}. \tag{21}$$

Now this problem is jointly convex w.r.t. (y, z) , by first-order optimality condition, we need to solve

$$\begin{cases} 0 \in \partial g(z) + \frac{1}{\lambda}(z - y) \\ \frac{1}{\lambda}(y - z) + \frac{1}{\gamma}(y - x) = 0. \end{cases}$$

Substituting $y = \frac{\gamma}{\gamma+\lambda}z + \frac{\lambda}{\gamma+\lambda}x$ from the second equation to the first equation, $z = \text{Prox}_{(\gamma+\lambda)g}(x)$. \square

Lemma 11. *Let $q \in \mathbb{N}^*$ and $q \geq 2$. There exists $C_q \in \mathbb{R}$ such that for all $x, z \in \mathbb{R}^d$ such that*

$$\|x + z\|^q \leq \|x\|^q + q\|x\|^{q-2}\langle x, z \rangle + C_q(\|x\|^{q-2}\|z\|^2 + \|z\|^q).$$

Proof. Let $\phi(u) = \|u\|^q$ and $g(t) = \phi(x + tz) = \|x + tz\|^q$. We have

$$g(1) = g(0) + g'(0) + \int_0^1 g''(t)(1-t)dt.$$

Now that

$$\begin{aligned} \nabla \phi(u) &= q\|u\|^{q-2}u \\ \nabla^2 \phi(u) &= q\|u\|^{q-2}I + q(q-2)\|u\|^{q-4}uu^\top, \quad u \neq 0, \end{aligned}$$

and $\nabla^2 \phi(0) = 2I$ if $q = 2$ and $\nabla^2 \phi(0) = 0$ if $q > 2$. It follows

$$\begin{aligned} g'(0) &= \langle \nabla \phi(x), z \rangle = q\|x\|^{q-2}\langle x, z \rangle, \\ g''(t) &= z^\top \nabla^2 \phi(x + tz)z \\ &= z^\top \left(q\|x + tz\|^{q-2}I + q(q-2)\|x + tz\|^{q-4}(x + tz)(x + tz)^\top \right) z \\ &= q\|x + tz\|^{q-2}\|z\|^2 + q(q-2)\|x + tz\|^{q-4}\langle z, x + tz \rangle^2. \end{aligned}$$

We evaluate

$$\begin{aligned} g''(t) &\leq q\|x + tz\|^{q-2}\|z\|^2 + q(q-2)\|x + tz\|^{q-2}\|z\|^2 \\ &= q(q-1)\|x + tz\|^{q-2}\|z\|^2. \end{aligned}$$

We have $\|x + tz\| \leq \|x\| + \|z\|$ for $t \in [0, 1]$ and

$$(\|x\| + \|z\|)^{q-2} \leq 2^{q-3}(\|x\|^{q-2} + \|z\|^{q-2})$$

where the inequality is an equality for $q \in \{2, 3\}$ and follows from Hölder inequality for $q \geq 4$. Therefore,

$$g''(t) \leq q(q-1)2^{q-3}(\|x\|^{q-2}\|z\|^2 + \|z\|^q),$$

it follows

$$\int_0^1 (1-s)g''(s)ds \leq q(q-1)2^{q-4}(\|x\|^{q-2}\|z\|^2 + \|z\|^q).$$

Putting together,

$$\|x + z\|^q \leq \|x\|^q + q\|x\|^{q-2}\langle x, z \rangle + q(q-1)2^{q-4}(\|x\|^{q-2}\|z\|^2 + \|z\|^q).$$

\square

Lemma 12. Let $\{Y_k\}_k$ be given by

$$Y_{k+1} = Y_k - \gamma b(Y_k) + \sqrt{2\gamma} Z_{k+1}$$

where $\{Z_k\}_k$ follows i.i.d. normal distribution and b is L -Lipschitz and (m, R) -distant dissipative. Suppose that $\gamma \leq \frac{m}{L^2}$. Let Q be the transition Markov kernel of $\{Y_k\}_k$, then Q has an invariant distribution $\pi_Y \in \mathcal{P}_1(\mathbb{R}^d)$. Furthermore, for $p' \geq 2, p' \in \mathbb{N}^*$, if γ is sufficiently small, i.e.,

$$\gamma \leq \min \left\{ \frac{1}{4L}, \frac{m}{2^{p'+2} L^2 (p' - 1)} \right\} \quad (22)$$

it holds $\pi_Y \in \mathcal{P}_{p'}(\mathbb{R}^d)$.

Proof. Since b is Lipschitz, similar to Subsection B, once the chain starts in $\mathcal{P}_{p'}(\mathbb{R}^d)$, it stays in $\mathcal{P}_p(\mathbb{R}^d)$. Theorem 5 in [Renaud et al., 2025a] guarantees that: there exist $D > 0, \rho \in (0, 1)$:

$$W_1(\mu Q^k, \nu Q^k) \leq D \rho^{k\gamma} W_1(\mu, \nu) \quad (23)$$

for all $\mu, \nu \in \mathcal{P}_1(\mathbb{R})$. Therefore, for large enough k , Q^k is contractive in $(\mathcal{P}_1(\mathbb{R}^d), W_1)$. Applying Picard fixed point theorem, for some fixed large k , there exists unique $\pi_Y \in \mathcal{P}_1(\mathbb{R}^d)$ such that $\pi_Y Q^k = \pi_Y$. It follows that $(\pi_Y Q)Q^k = \pi_Y Q$ and by uniqueness $\pi_Y Q = \pi_Y$. If $p' = 1$, the proof is complete. For $p' \geq 2$, we need to further show $\pi_Y \in \mathcal{P}_{p'}(\mathbb{R}^d)$ when γ satisfies (22). Since b is L -Lipschitz,

$$\|b(x)\| \leq L\|x\| + \|b(0)\| := L\|x\| + a, \quad \forall x.$$

b being (m, R) -distant dissipative implies

$$\langle b(x), x \rangle \geq \frac{m}{2}\|x\|^2 - \frac{1}{2m}\|b(0)\|^2 \quad \forall x : \|x\| \geq R.$$

So there exists $c > 0$:

$$\langle b(x), x \rangle \geq \frac{m}{2}\|x\|^2 - c, \quad \forall x \in \mathbb{R}^d. \quad (24)$$

We have

$$\mathbb{E}(\|Y_{k+1}\|^{p'} | Y_k = y) = \mathbb{E}\|y - \gamma b(y) + \sqrt{2\gamma} Z\|^{p'},$$

where $Z \sim \mathcal{N}(0, I)$. Applying Lemma 11, there exists $C_{p'}$ such that

$$\|x + z\|^{p'} \leq \|x\|^{p'} + p'\|x\|^{p'-2}\langle x, z \rangle + C_{p'}(\|x\|^{p'-2}\|z\|^2 + \|z\|^{p'}).$$

Therefore,

$$\begin{aligned} \|y - \gamma b(y) + \sqrt{2\gamma} Z\|^{p'} &\leq \|y\|^{p'} + p'\|y\|^{p'-2}\langle y, -\gamma b(y) + \sqrt{2\gamma} Z \rangle \\ &\quad + C_{p'}(\|y\|^{p'-2}\|-\gamma b(y) + \sqrt{2\gamma} Z\|^2 + \|\gamma b(y) + \sqrt{2\gamma} Z\|^{p'}) \end{aligned}$$

so

$$\begin{aligned} \mathbb{E}\|y - \gamma b(y) + \sqrt{2\gamma} Z\|^{p'} &\leq \|y\|^{p'} - \gamma p'\|y\|^{p'-2}\langle y, b(y) \rangle \\ &\quad + C_{p'}\|y\|^{p'-2}\mathbb{E}\|-\gamma b(y) + \sqrt{2\gamma} Z\|^2 + C_{p'}\mathbb{E}\|\gamma b(y) + \sqrt{2\gamma} Z\|^{p'}. \end{aligned}$$

Now use (24),

$$\begin{aligned} \mathbb{E}\|y - \gamma b(y) + \sqrt{2\gamma} Z\|^{p'} &\leq \|y\|^{p'} + \gamma p'\|y\|^{p'-2}\left(-\frac{m}{2}\|y\|^2 + c\right) + 2C_{p'}\|y\|^{p'-2}(\gamma^2\|b(y)\|^2 + 2\gamma d) \\ &\quad + C_{p'}\mathbb{E}\left(\gamma\|b(y)\| + \sqrt{2\gamma}\|Z\|\right)^{p'}. \end{aligned}$$

Applying Hölder inequality

$$\left(\gamma\|b(y)\| + \sqrt{2\gamma}\|Z\|\right)^{p'} \leq 2^{p'-1} \left(\gamma^{p'}\|b(y)\|^{p'} + (2\gamma)^{\frac{p'}{2}}\|Z\|^{p'}\right),$$

we get

$$\begin{aligned} & \mathbb{E}\|y - \gamma b(y) + \sqrt{2\gamma}Z\|^{p'} \\ & \leq \|y\|^{p'} + \gamma p'\|y\|^{p'-2} \left(-\frac{m}{2}\|y\|^2 + c\right) + 2C_{p'}\|y\|^{p'-2}(\gamma^2\|b(y)\|^2 + 2\gamma d) \\ & \quad + C_{p'}\gamma^{p'}2^{p'-1}\|b(y)\|^{p'} + 2^{\frac{3p'}{2}-1}C_{p'}\gamma^{\frac{p'}{2}}\mathbb{E}\|Z\|^{p'} \\ & = \|y\|^{p'} - \frac{m\gamma p'}{2}\|y\|^{p'} + 2C_{p'}\gamma^2\|y\|^{p'-2}\|b(y)\|^2 + 4C_{p'}\gamma d\|y\|^{p'-2} + c\gamma p'\|y\|^{p'-2} \\ & \quad + C_{p'}\gamma^{p'}2^{p'-1}\|b(y)\|^{p'} + 2^{\frac{3p'}{2}-1}C_{p'}\gamma^{\frac{p'}{2}}\mathbb{E}\|Z\|^{p'}. \end{aligned}$$

Now use $\|b(y)\| \leq L\|y\| + a$, it holds

$$\begin{aligned} \|b(y)\|^2 & \leq 2(L^2\|y\|^2 + a^2) \\ \|b(y)\|^{p'} & \leq 2^{p'-1}(L^{p'}\|y\|^{p'} + a^{p'}). \end{aligned}$$

Then

$$\begin{aligned} \mathbb{E}\|y - \gamma b(y) + \sqrt{2\gamma}Z\|^{p'} & \leq \left(1 + 4C_{p'}\gamma^2L^2 + C_{p'}\gamma^{p'}2^{2p'-2}L^{p'} - \frac{m\gamma p'}{2}\right)\|y\|^{p'} \\ & \quad + (4C_{p'}\gamma d + 4C_{p'}\gamma^2a^2 + c\gamma p')\|y\|^{p'-2} + C_{p'}\gamma^{p'}2^{2p'-2}a^{p'} + 2^{\frac{3p'}{2}-1}C_{p'}\gamma^{\frac{p'}{2}}\mathbb{E}\|Z\|^{p'}. \end{aligned} \quad (25)$$

Taking expectation over $y \sim p_{Y_k}$, we get

$$\begin{aligned} \mathbb{E}\|Y_{k+1}\|^{p'} & \leq \left(1 + 4C_{p'}\gamma^2L^2 + C_{p'}\gamma^{p'}2^{2p'-2}L^{p'} - \frac{m\gamma p'}{2}\right)\mathbb{E}\|Y_k\|^{p'} \\ & \quad + (4C_{p'}\gamma d + 4C_{p'}\gamma^2a^2 + c\gamma p')\mathbb{E}\|Y_k\|^{p'-2} + C_{p'}\gamma^{p'}2^{2p'-2}a^{p'} + 2^{\frac{3p'}{2}-1}C_{p'}\gamma^{\frac{p'}{2}}\mathbb{E}\|Z\|^{p'}. \end{aligned} \quad (26)$$

Let $\bar{R} > 0$ so that

$$\bar{R}^2 \geq 4 \frac{4C_{p'}\gamma d + 4C_{p'}\gamma^2a^2 + c\gamma p'}{m\gamma p'}. \quad (27)$$

We have

$$\|y\|^{p'-2} \leq \frac{\|y\|^{p'}}{\bar{R}^2} \quad \text{for } \|y\| \geq \bar{R}.$$

So

$$\begin{aligned} \mathbb{E}\|Y_k\|^{p'-2} & = \int_{\|y\| \geq \bar{R}} \|y\|^{p'-2} p_{Y_k}(y) dy + \int_{\|y\| \leq \bar{R}} \|y\|^{p'-2} p_{Y_k}(y) dy \\ & \leq \frac{1}{\bar{R}^2} \int_{\|y\| \geq \bar{R}} \|y\|^{p'} p_{Y_k}(y) dy + \bar{R}^{p'-2} \\ & \leq \frac{1}{\bar{R}^2} \mathbb{E}\|Y_k\|^{p'} + \bar{R}^{p'-2}. \end{aligned}$$

Applying this inequality to (26), and thanks to (27), we obtain that

$$\begin{aligned}
\mathbb{E}\|Y_{k+1}\|^{p'} &\leq \left(1 + 4C_{p'}\gamma^2L^2 + C_{p'}\gamma^{p'}2^{2p'-2}L^{p'} - \frac{m\gamma p'}{2} + \frac{4C_{p'}\gamma d + 4C_{p'}\gamma^2a^2 + c\gamma p'}{\bar{R}^2}\right)\mathbb{E}\|Y_k\|^{p'} \\
&\quad + (4C_{p'}\gamma d + 4C_{p'}\gamma^2a^2 + c\gamma p')\bar{R}^{p'-2} + C_{p'}\gamma^{p'}2^{2p'-2}a^{p'} + 2^{\frac{3p'}{2}-1}C_{p'}\gamma^{\frac{p'}{2}}\mathbb{E}\|Z\|^{p'} \\
&\leq \left(1 + 4C_{p'}\gamma^2L^2 + C_{p'}\gamma^{p'}2^{2p'-2}L^{p'} - \frac{m\gamma p'}{4}\right)\mathbb{E}\|Y_k\|^{p'} \\
&\quad + (4C_{p'}\gamma d + 4C_{p'}\gamma^2a^2 + c\gamma p')\bar{R}^{p'-2} + C_{p'}\gamma^{p'}2^{2p'-2}a^{p'} + 2^{\frac{3p'}{2}-1}C_{p'}\gamma^{\frac{p'}{2}}\mathbb{E}\|Z\|^{p'}.
\end{aligned} \tag{28}$$

Now for γ small enough as in (22), it holds

$$1 + 4C_{p'}\gamma^2L^2 + C_{p'}\gamma^{p'}2^{2p'-2}L^{p'} - \frac{m\gamma p'}{4} < 1. \tag{29}$$

By choosing $Y_1 \in \mathcal{P}_{p'}(\mathbb{R}^d)$, the recursion (28) and (29) imply

$$\sup_k \mathbb{E}\|Y_k\|^{p'} < +\infty.$$

From (23), setting $\nu = \pi_Y$ we get p_{Y_k} converging to π_Y in 1-Wasserstein, which further implies *narrow convergence*, i.e., for any φ bounded and continuous, it holds

$$\int \varphi(y)p_{Y_k}(y)dy \rightarrow \int \varphi(y)\pi_Y(y)dy.$$

Let $\varphi_M(y) := \min\{\|y\|^{p'}, M\}$,

$$\int \varphi_M(y)\pi_Y(y)dy = \lim_{k \rightarrow \infty} \int \varphi_M(y)p_{Y_k}(y)dy \leq \sup_k \int \|y\|^{p'} p_{Y_k}(y)dy = \sup_k \mathbb{E}\|Y_k\|^{p'} < +\infty.$$

By letting $M \rightarrow \infty$ and applying the monotone convergence theorem, we obtain

$$\int \|y\|^{p'} \pi_Y(y)dy < +\infty.$$

□

I Proofs

I.1 Proof of Lemma 4

1) Suppose that for all $\|x - y\| \geq R$,

$$\langle \nabla f(x) + \partial r_1(x) - \partial r_2(x) - \nabla f(y) - \partial r_1(y) + \partial r_2(y), x - y \rangle \geq \mu\|x - y\|^2.$$

Here, by abuse of notation we still use the set notation ∂ in the above inequality.

It follows that

$$\begin{aligned}
\langle \nabla f(x) - \nabla f(y), x - y \rangle &\geq \mu\|x - y\|^2 - \langle \partial r_1(x) - \partial r_1(y), x - y \rangle + \langle \partial r_2(x) - \partial r_2(y), x - y \rangle \\
&\geq \mu\|x - y\|^2 - \langle \partial r_1(x) - \partial r_1(y), x - y \rangle \\
&\geq \mu\|x - y\|^2 - 2G_1\|x - y\|.
\end{aligned}$$

Therefore, f is $(\frac{\mu}{2}, \bar{R})$ distant dissipative where $\bar{R} = \max\{R, 4G_1/\mu\}$.

2) Suppose that for all $\|x - y\| \geq R$,

$$\langle \nabla f(x) - \nabla f(y), x - y \rangle \geq \mu\|x - y\|^2.$$

Then

$$\begin{aligned}
& \langle \nabla f(x) + \partial r_1(x) - \partial r_2(x) - \nabla f(y) - \partial r_1(y) + \partial r_2(y), x - y \rangle \\
& \geq \mu \|x - y\|^2 - \langle \partial r_2(x) - \partial r_2(y), x - y \rangle \\
& \geq \begin{cases} \mu \|x - y\|^2 - 2G_2 \|x - y\| & \text{if Assumption 4(i)} \\ \mu \|x - y\|^2 - M \|x - y\|^{\kappa+1} & \text{if Assumption 4(ii).} \end{cases}
\end{aligned}$$

Therefore, V is $(\frac{\mu}{2}, \bar{R})$ -distant dissipative where $\bar{R} = \max\{R, 4G_2/\mu\}$ if Assumption 4(i), $\max\{R, (2M/\mu)^{\frac{1}{1-\kappa}}\}$ if Assumption 4(ii).

I.2 Proof of Lemma 5

We write

$$Y_{k+1} = \text{Prox}_{\gamma r_1^\lambda}(Y_k) - \gamma \nabla f(\text{Prox}_{\gamma r_1^\lambda}(Y_k)) + \gamma \nabla r_2^\lambda(\text{Prox}_{\gamma r_1^\lambda}(Y_k)) + \sqrt{2\gamma} Z_{k+1}. \quad (30)$$

Now using $\text{Prox}_{\gamma r_1^\lambda}(Y_k) = Y_k - \gamma \nabla(r_1^\lambda)^\gamma(Y_k)$, we get

$$Y_{k+1} = Y_k - \gamma \nabla(r_1^\lambda)^\gamma(Y_k) - \gamma \nabla f(\text{Prox}_{\gamma r_1^\lambda}(Y_k)) + \gamma \nabla r_2^\lambda(\text{Prox}_{\gamma r_1^\lambda}(Y_k)) + \sqrt{2\gamma} Z_{k+1}. \quad (31)$$

Since $\nabla(r_1^\lambda)^\gamma(Y_k) = \nabla r_1^\lambda(\text{Prox}_{\gamma r_1^\lambda}(Y_k))$,

$$Y_{k+1} = Y_k - \gamma \nabla r_1^\lambda(\text{Prox}_{\gamma r_1^\lambda}(Y_k)) - \gamma \nabla f(\text{Prox}_{\gamma r_1^\lambda}(Y_k)) + \gamma \nabla r_2^\lambda(\text{Prox}_{\gamma r_1^\lambda}(Y_k)) + \sqrt{2\gamma} Z_{k+1}.$$

Now since r_i^λ is $\frac{1}{\lambda}$ -smooth for $i \in \{1, 2\}$, it holds

$$\|\nabla r_i^\lambda(\text{Prox}_{\gamma r_1^\lambda}(x)) - \nabla r_i^\lambda(\text{Prox}_{\gamma r_1^\lambda}(y))\| \leq \frac{1}{\lambda} \|\text{Prox}_{\gamma r_1^\lambda}(x) - \text{Prox}_{\gamma r_1^\lambda}(y)\| \leq \frac{1}{\lambda} \|x - y\|,$$

where the last inequality is thanks to the nonexpansiveness of the proximal operator. Therefore, for all $\gamma > 0$, $\nabla r_i^\lambda(\text{Prox}_{\gamma r_1^\lambda}(x))$ is $\frac{1}{\lambda}$ -Lipschitz. As f is L_f -smooth, the drift b_λ^γ is $(\frac{2}{\lambda} + L_f)$ -Lipschitz.

I.3 Proof of Lemma 6

$$\begin{aligned}
& \langle b_\lambda^\gamma(x) - b_\lambda^\gamma(y), x - y \rangle \\
& = \left\langle \nabla r_1^\lambda(\text{Prox}_{\gamma r_1^\lambda}(x)) + \nabla f(\text{Prox}_{\gamma r_1^\lambda}(x)) - \nabla r_2^\lambda(\text{Prox}_{\gamma r_1^\lambda}(x)) \right. \\
& \quad \left. - \nabla r_1^\lambda(\text{Prox}_{\gamma r_1^\lambda}(y)) - \nabla f(\text{Prox}_{\gamma r_1^\lambda}(y)) + \nabla r_2^\lambda(\text{Prox}_{\gamma r_1^\lambda}(y)), x - y \right\rangle \\
& = \underbrace{\langle \nabla r_1^\lambda(\text{Prox}_{\gamma r_1^\lambda}(x)) - \partial r_1(x) - \nabla r_1^\lambda(\text{Prox}_{\gamma r_1^\lambda}(y)) + \partial r_1(y), x - y \rangle}_{:=I} + \\
& \quad + \underbrace{\langle \nabla f(\text{Prox}_{\gamma r_1^\lambda}(x)) - \nabla f(x) - \nabla f(\text{Prox}_{\gamma r_1^\lambda}(y)) + \nabla f(y), x - y \rangle}_{:=II} \\
& \quad + \underbrace{\langle -\nabla r_2^\lambda(\text{Prox}_{\gamma r_1^\lambda}(x)) + \partial r_2(x) + \nabla r_2^\lambda(\text{Prox}_{\gamma r_1^\lambda}(y)) - \partial r_2(y), x - y \rangle}_{:=III} \\
& \quad + \underbrace{\langle \partial r_1(x) - \partial r_1(y) + \nabla f(x) - \nabla f(y) - \partial r_2(x) + \partial r_2(y), x - y \rangle}_{:=IV}
\end{aligned}$$

The first term:

$$I \geq - \left(\|\nabla r_1^\lambda(\text{Prox}_{\gamma r_1^\lambda}(x))\| + \|\partial r_1(x)\| + \|\nabla r_1^\lambda(\text{Prox}_{\gamma r_1^\lambda}(y))\| + \|\partial r_1(y)\| \right) \|x - y\|.$$

Since $\nabla r_1^\lambda(\text{Prox}_{\gamma r_1^\lambda}(x)) \in \partial r_1(\text{Prox}_{\lambda r_1}(\text{Prox}_{\gamma r_1^\lambda}(x)))$, under Assumption 3, it holds

$$I \geq -4G_1\|x - y\|.$$

The second term,

$$\begin{aligned} II &\geq -\|\nabla f(\text{Prox}_{\gamma r_1^\lambda}(x)) - \nabla f(x) - \nabla f(\text{Prox}_{\gamma r_1^\lambda}(y)) + \nabla f(y)\|\|x - y\| \\ &\geq -L_f \left(\|\text{Prox}_{\gamma r_1^\lambda}(x) - x\| + \|\text{Prox}_{\gamma r_1^\lambda}(y) - y\| \right) \|x - y\|. \end{aligned}$$

Now that

$$\begin{aligned} x - \text{Prox}_{\gamma r_1^\lambda}(x) &= \gamma \nabla(r_1^\lambda)^\gamma(x) = \gamma \nabla r_1^\lambda(\text{Prox}_{\gamma r_1^\lambda}(x)) \\ &\in \gamma \partial r_1(\text{Prox}_{\lambda r_1}(\text{Prox}_{\gamma r_1^\lambda}(x))). \end{aligned} \quad (32)$$

Therefore,

$$II \geq -2L_f \gamma G_1 \|x - y\|.$$

The third term:

$$III \geq \langle -\nabla r_2^\lambda(\text{Prox}_{\gamma r_1^\lambda}(x)) + \nabla r_2^\lambda(\text{Prox}_{\gamma r_1^\lambda}(y)), x - y \rangle.$$

Under Assumption 4, if case (i) happens, we have

$$III \geq -2G_2\|x - y\|,$$

and if case (ii) happens

$$\begin{aligned} III &\geq -\|\nabla r_2(\text{Prox}_{\lambda r_2}(\text{Prox}_{\gamma r_1^\lambda}(x))) - \nabla r_2(\text{Prox}_{\lambda r_2}(\text{Prox}_{\gamma r_1^\lambda}(y)))\|\|x - y\| \\ &\geq -M\|\text{Prox}_{\lambda r_2}(\text{Prox}_{\gamma r_1^\lambda}(x)) - \text{Prox}_{\lambda r_2}(\text{Prox}_{\gamma r_1^\lambda}(y))\|^\kappa\|x - y\| \\ &\geq -M\|\text{Prox}_{\gamma r_1^\lambda}(x) - \text{Prox}_{\gamma r_1^\lambda}(y)\|^\kappa\|x - y\| \\ &\geq -M\|x - y\|^{\kappa+1}. \end{aligned}$$

The last term: if $\|x - y\| \geq R_0$

$$IV \geq \mu\|x - y\|^2$$

thanks to the Assumption 2. From these evaluations, we get

$$\begin{aligned} &\langle b_\lambda^\gamma(x) - b_\lambda^\gamma(y), x - y \rangle \\ &\geq \begin{cases} \mu\|x - y\|^2 - (4G_1 + 2L_f \gamma G_1 + 2G_2)\|x - y\| & \text{if Assumption 4(i)} \\ \mu\|x - y\|^2 - (4G_1 + 2L_f \gamma G_1)\|x - y\| - M\|x - y\|^{\kappa+1} & \text{if Assumption 4(ii).} \end{cases} \end{aligned}$$

For $\|x - y\|$ being large, the second-order term dominates the lower-order terms (note that $\kappa < 1$), we get:

$$\langle b_\lambda^\gamma(x) - b_\lambda^\gamma(y), x - y \rangle \geq \frac{\mu}{2}\|x - y\|^2 \quad (33)$$

whenever

$$\|x - y\| \geq \begin{cases} \max \left\{ R_0, \frac{8G_1 + 4L_f \gamma_0 G_1 + 4G_2}{\mu} \right\} & \text{if Assumption 4(i)} \\ \max \left\{ R_0, \frac{16G_1 + 8L_f \gamma_0 G_1}{\mu}, \left(\frac{4M}{\mu} \right)^{\frac{1}{1-\kappa}} \right\} & \text{if Assumption 4(ii).} \end{cases} \quad (34)$$

I.4 Proof of the distant dissipativity of \bar{b}_λ^γ

For $\|x - y\| \geq R_0$,

$$\begin{aligned}
& \langle \bar{b}_\lambda^\gamma(x) - \bar{b}_\lambda^\gamma(y), x - y \rangle \\
&= \langle \nabla r_1^\lambda(\text{Prox}_{\gamma r_1^\lambda}(x)) + \nabla f(x) - \nabla r_2^\lambda(x) - \nabla r_1^\lambda(\text{Prox}_{\gamma r_1^\lambda}(y)) - \nabla f(y) + \nabla r_2^\lambda(y), x - y \rangle \\
&= \langle \nabla r_1^\lambda(\text{Prox}_{\gamma r_1^\lambda}(x)) - \partial r_1(x) - \nabla r_1^\lambda(\text{Prox}_{\gamma r_1^\lambda}(y)) + \partial r_1(y), x - y \rangle \\
&\quad + \langle -\nabla r_2^\lambda(x) + \partial r_2(x) + \nabla r_2^\lambda(y) - \partial r_2(y), x - y \rangle \\
&\quad + \langle \partial r_1(x) + \nabla f(x) - \partial r_2(x) - \partial r_1(y) - \nabla f(y) + \partial r_2(y), x - y \rangle \\
&\geq -4G_1\|x - y\| + \langle -\nabla r_2^\lambda(x) + \nabla r_2^\lambda(y), x - y \rangle + \mu\|x - y\|^2.
\end{aligned}$$

Therefore,

$$\langle \bar{b}_\lambda^\gamma(x) - \bar{b}_\lambda^\gamma(y), x - y \rangle \geq \begin{cases} \mu\|x - y\|^2 - (4G_1 + 2G_2)\|x - y\| & \text{if Assumption 4(i)} \\ \mu\|x - y\|^2 - 4G_1\|x - y\| - M\|x - y\|^{\kappa+1} & \text{if Assumption 4(ii).} \end{cases}$$

where the last inequality follows the same arguments as in the proof of Lemma 6 (Appendix I.3).

Therefore,

$$\langle \bar{b}_\lambda^\gamma(x) - \bar{b}_\lambda^\gamma(y), x - y \rangle \geq \frac{\mu}{2}\|x - y\|^2$$

whenever

$$\|x - y\| \geq \begin{cases} \max \left\{ R_0, \frac{8G_1 + 4G_2}{\mu} \right\} & \text{if Assumption 4(i)} \\ \max \left\{ R_0, \frac{16G_1}{\mu}, \left(\frac{4M}{\mu} \right)^{\frac{1}{1-\kappa}} \right\} & \text{if Assumption 4(ii).} \end{cases}$$

I.5 Proof of Theorem 7

Let Q, \bar{Q} be transition kernels of $\{Y_k\}_k$ and $\{\bar{Y}_k\}_k$, respectively. Recall that

$$Y_1 = X_0 - \gamma \nabla f(X_0) + \gamma \nabla r_2^\lambda(X_0) + \sqrt{2\gamma} Z_1.$$

In Appendix B, we show that: if $X_0 \in \mathcal{P}_{p'}(\mathbb{R}^d)$ for some $p' \geq 1$, then $Y_1 \in \mathcal{P}_{p'}(\mathbb{R}^d)$. By assumption, $X_0 \in \mathcal{P}_1(\mathbb{R}^d)$ if $q = 1$ and $X_0 \in \mathcal{P}_{2q}(\mathbb{R}^d)$ if $q \geq 2$. So $Y_1 \in \mathcal{P}_1(\mathbb{R}^d)$ if $q = 1$ and $Y_1 \in \mathcal{P}_{2q}(\mathbb{R}^d)$ if $q \geq 2$. Furthermore, applying Lemma 12 (for $p' = 2q$), there exist invariant distributions of Q and \bar{Q} named $p_{\lambda,\gamma}, \bar{p}_{\lambda,\gamma}$ in $\mathcal{P}_1(\mathbb{R}^d)$ and further in $\mathcal{P}_{2q}(\mathbb{R}^d)$ if $q \geq 2$.

We now consider two cases $q = 1$ and $q \geq 2$ separately since they require slightly different conditions.

Case 1: $q = 1$

Renaud et al. [2025a] showed in the proof of Theorem 5 that: there exist $D(\lambda) > 0$ and $\rho_\lambda \in (0, 1)$ so that

$$W_1(\nu_1 Q^k, \nu_2 Q^k) \leq D(\lambda) \rho_\lambda^{k\gamma} W_1(\nu_1, \nu_2)$$

where $\nu_1, \nu_2 \in \mathcal{P}_1(\mathbb{R}^d)$ are two initial distributions.

Plugging $\nu_1 := p_{\lambda,\gamma}$ the invariant distribution of Q and $\nu_2 := p_{Y_1}$ the initial distribution of the chain, we get

$$W_1(p_{\lambda,\gamma}, p_{Y_{k+1}}) \leq D(\lambda) \rho_\lambda^{k\gamma} W_1(p_{\lambda,\gamma}, p_{Y_1}).$$

We will show that: $W_1(p_{\lambda,\gamma}, p_{Y_1})$ is uniformly bounded by a constant that does not depend on γ , i.e., there exist $C_1(\lambda) > 0, \rho_\lambda \in (0, 1)$,

$$W_1(p_{\lambda,\gamma}, p_{Y_{k+1}}) \leq C_1(\lambda) \rho_\lambda^{k\gamma}, \quad \forall k \in \mathbb{N}. \quad (35)$$

We defer the proof of (35) to a later part of the text.

Now [Renaud et al., 2025a, Theorem 1] states that: there exists $C_2(\lambda)$ such that

$$W_1(p_{\lambda,\gamma}, \bar{p}_{\lambda,\gamma}) \leq C_2(\lambda) \left(\mathbb{E}_{X \sim p_{\lambda,\gamma}} \|b_\lambda^\gamma(X) - \bar{b}_\lambda^\gamma(X)\|^2 \right)^{\frac{1}{2}}. \quad (36)$$

On the other hand,

$$\|b_\lambda^\gamma(y) - \bar{b}_\lambda^\gamma(y)\| \leq \left(L_f + \frac{1}{\lambda} \right) \|\text{Prox}_{\gamma r_1^\lambda}(y) - y\| \leq \left(L_f + \frac{1}{\lambda} \right) G_1 \gamma \quad (37)$$

where the last inequality is thanks to (32). Therefore,

$$W_1(p_{\lambda,\gamma}, \bar{p}_{\lambda,\gamma}) \leq C_2(\lambda) \left(L_f + \frac{1}{\lambda} \right) G_1 \gamma. \quad (38)$$

At the same time, thanks to [Renaud et al., 2025a, Theorem 2], there exists $C_3(\lambda) > 0$ such that:

$$W_1(\bar{p}_{\lambda,\gamma}, \pi_{\lambda,\gamma}) \leq C_3(\lambda) \gamma^{\frac{1}{2}} \quad (39)$$

where $\pi_{\lambda,\gamma}$ is defined in (14).

From (35), (38), and (39),

$$W_1(p_{Y_{k+1}}, \pi_{\lambda,\gamma}) \leq C_1(\lambda) \rho_\lambda^{k\gamma} + C_2(\lambda) \left(L_f + \frac{1}{\lambda} \right) G_1 \gamma + C_3(\lambda) \gamma^{\frac{1}{2}}. \quad (40)$$

Here we can denote $A_\lambda = C_1(\lambda), B_\lambda = C_2(\lambda) \left(L_f + \frac{1}{\lambda} \right) G_1 \gamma_0^{\frac{1}{2}} + C_3(\lambda)$ for some γ_0 being an upper bound of γ .

The above result gives a convergence guarantee to $\pi_{\lambda,\gamma}$ for the law of the sequence $\{Y_k\}$. As promised, we prove (35) by uniformly bounding $W_1(p_{\lambda,\gamma}, p_{Y_1})$ as follows. We have

$$\begin{aligned} W_1(p_{\lambda,\gamma}, p_{Y_1}) &\leq W_1(p_{\lambda,\gamma}, \bar{p}_{\lambda,\gamma}) + W_1(\bar{p}_{\lambda,\gamma}, \pi_{\lambda,\gamma}) + W_1(\pi_{\lambda,\gamma}, p_{Y_1}) \\ &\leq C_2(\lambda) \left(L_f + \frac{1}{\lambda} \right) G_1 \gamma_0 + C_3(\lambda) \gamma_0^{\frac{1}{2}} + W_1(\pi_{\lambda,\gamma}, p_{Y_1}) \end{aligned}$$

where γ_0 denotes the upper bound of γ (the step size condition in Theorem 7). On the other hand, from (18), it holds

$$\pi_{\lambda,\gamma}(x) \leq e^{\frac{G_1^2 \gamma_0}{2}} \pi_\lambda(x). \quad (41)$$

So,

$$\begin{aligned} W_1(\pi_{\lambda,\gamma}, p_{Y_1}) &\leq \int \|x\| \pi_{\lambda,\gamma}(x) dx + \int \|x\| p_{Y_1}(x) dx \\ &\leq e^{\frac{G_1^2 \gamma_0}{2}} \int \|x\| \pi_\lambda(x) dx + \int \|x\| p_{Y_1}(x) dx. \end{aligned}$$

This is a uniform bound.

Now we turn to the original sequence $X_{k+1} = \text{Prox}_{\gamma r_1^\lambda}(Y_{k+1})$. The distribution of X_{k+1} is $p_{X_{k+1}} = (\text{Prox}_{\gamma r_1^\lambda})_\# p_{Y_{k+1}}$. Let $\nu_{\lambda,\gamma} = (\text{Prox}_{\gamma r_1^\lambda})_\# \pi_{\lambda,\gamma}$ and (X, Y) be the optimal coupling of $(\pi_{\lambda,\gamma}, p_{Y_{k+1}})$,

$$\begin{aligned} W_1(p_{X_{k+1}}, \nu_{\lambda,\gamma}) &\leq \mathbb{E} \|\text{Prox}_{\gamma r_1^\lambda}(X) - \text{Prox}_{\gamma r_1^\lambda}(Y)\| \\ &\leq \mathbb{E} \|X - Y\| \\ &= W_1(\pi_{\lambda,\gamma}, p_{Y_{k+1}}). \end{aligned}$$

Case 2: $q \geq 2$

According to the proof of Theorem 5 in [Renaud et al., 2025a] and Lemma 18 therein: there exist $D_q(\lambda) > 0, \rho_\lambda \in (0, 1)$:

$$W_q(\mu Q^k, \nu Q^k)^q \leq 2^{q-1} \|\mu Q^k - \nu Q^k\|_{V_q} \leq D_q(\lambda) \rho_\lambda^{k\gamma} (\mu(V_q^2) + \nu(V_q^2)).$$

where $V_q = 1 + \|\cdot\|^q$. In particular, with $\nu = p_{\lambda,\gamma}$, it holds

$$W_q(\mu Q^k, p_{\lambda,\gamma})^q \leq D_q(\lambda) \rho_\lambda^{k\gamma} (\mu(V_q^2) + p_{\lambda,\gamma}(V_q^2)). \quad (42)$$

Thanks to Lemma 12, $p_{\lambda,\gamma}(V_q^2) < +\infty$, the convergence is exponentially fast given that $\mu \in \mathcal{P}_{2q}(\mathbb{R}^d)$. From (42), we will further show the following uniform bound in the later part of the text: there exist $C_{1,q}(\lambda) > 0$:

$$W_q(p_{Y_{k+1}}, p_{\lambda,\gamma}) \leq C_{1,q}(\lambda) \rho_\lambda^{k\gamma/q}. \quad (43)$$

On another hand, from [Renaud et al., 2025a, Theorem 1], there exists $C_{2,q}(\lambda) > 0$

$$W_q(p_{\lambda,\gamma}, \bar{p}_{\lambda,\gamma}) \leq C_{2,q}(\lambda) \left(L_f + \frac{1}{\lambda} \right)^{\frac{1}{q}} (G_1 \gamma)^{\frac{1}{q}}$$

and from [Renaud et al., 2025a, Theorem 2], there exists $C_{3,q}(\lambda) > 0$:

$$W_q(\bar{p}_{\lambda,\gamma}, \pi_{\lambda,\gamma}) \leq C_{3,q}(\lambda) \gamma^{\frac{1}{2q}}.$$

Therefore,

$$W_q(p_{Y_{k+1}}, \pi_{\lambda,\gamma}) \leq C_{1,q}(\lambda) \rho_\lambda^{k\gamma/q} + C_{2,q}(\lambda) \left(L_f + \frac{1}{\lambda} \right)^{\frac{1}{q}} G_1^{\frac{1}{q}} \gamma^{\frac{1}{q}} + C_{3,q}(\lambda) \gamma^{\frac{1}{2q}}.$$

Note that the convergence rate in the theorem is then $\rho_\lambda^{1/q} \in (0, 1)$. Here, by abuse of notation, we still denote this rate by ρ_λ .

Finally, we show the uniform bound (43) which boils down to a uniform bound for $p_{\lambda,\gamma}(V_{2q})$. We have

$$W_{2q}(p_{\lambda,\gamma}, \pi_{\lambda,\gamma}) \leq W_{2q}(p_{\lambda,\gamma}, \bar{p}_{\lambda,\gamma}) + W_{2q}(\bar{p}_{\lambda,\gamma}, \pi_{\lambda,\gamma}). \quad (44)$$

Similar to the arguments of Case 1, the RHS of (44) can be bounded uniformly by some $E(\lambda)$. By Hölder inequality,

$$\|x\|^{2q} \leq 2^{2q-1} (\|y\|^{2q} + \|x - y\|^{2q}).$$

Let (X, Y) be the optimal coupling w.r.t. the cost $d(x, y) = \|x - y\|^{2q}$ of $p_{\lambda, \gamma}$ and $\pi_{\lambda, \gamma}$,

$$\begin{aligned}
\int \|x\|^{2q} dp_{\lambda, \gamma}(x) &= \mathbb{E} \|X\|^{2q} \\
&\leq 2^{2q-1} (\mathbb{E} \|Y\|^{2q} + \mathbb{E} \|X - Y\|^{2q}) \\
&= 2^{2q-1} (\mathbb{E} \|Y\|^{2q} + W_{2q}(p_{\lambda, \gamma}, \pi_{\lambda, \gamma})^{2q}) \\
&\leq 2^{2q-1} \left(\int \|y\|^{2q} d\pi_{\lambda, \gamma}(y) + E(\lambda)^{2q} \right) \\
&\leq 2^{2q-1} \left(e^{\frac{G_1^2 \gamma_0}{2}} \int \|y\|^{2q} d\pi_\lambda(y) + E(\lambda)^{2q} \right)
\end{aligned}$$

where the last inequality follows (41).

Lastly, for the sequence $\{X_k\}_k$

$$W_q(p_{X_{k+1}}, \nu_{\lambda, \gamma}) \leq W_q(p_{Y_{k+1}}, \pi_{\lambda, \gamma}).$$

I.6 On the dependence on λ

We discuss the behavior of A_λ , B_λ and ρ_λ w.r.t. λ at the limit of 0. We consider the case $q = 1$ for simplicity.

Retrieving constants from [De Bortoli and Durmus, 2019] and note that we are in the regime of small λ , we get

$$\log(\log^{-1}(\rho_\lambda^{-1})) = \tilde{O}(1/\lambda)$$

and A_λ, B_λ behave like $O(e^{\frac{c}{\lambda}})$ for some $c > 0$ independent to λ .

I.7 Bound $W_q(\pi_\lambda, \pi)$

We follow the proof template in [Renaud et al., 2025a, Appendix G.3] where we additionally handle the part $-r^\lambda$.

Case 1: Assumption 4(i):

Since r_i is G_i -Lipschitz ($i \in \{1, 2\}$), it holds $r_i(x) - r_i^\lambda(x) \leq \frac{\lambda G_i^2}{2}$ for all x . Combining with the fact that the Moreau envelope of a function is a lower bound of that function, we get

$$-\frac{\lambda G_2^2}{2} \leq r_1 - r_2 - (r_1^\lambda - r_2^\lambda) \leq \frac{\lambda G_1^2}{2}. \quad (45)$$

Let $\beta := \frac{\lambda G_2^2}{2}$. Given a function $\mathcal{V} : \mathbb{R}^d \rightarrow [1, \infty)$ (that induces the \mathcal{V} -norm), we write

$$\begin{aligned}
\|\pi_\lambda - \pi\|_{\mathcal{V}} &= \sup_{|\phi| \leq \mathcal{V}} \int \phi(x)(\pi_\lambda(x) - \pi(x))dx \\
&\leq \sup_{|\phi| \leq \mathcal{V}} \int |\phi(x)| |\pi_\lambda(x) - \pi(x)| dx \\
&\leq \int \mathcal{V}(x) |\pi_\lambda(x) - \pi(x)| dx \\
&= \int \mathcal{V}(x) \pi(x) \left| 1 - \frac{\pi_\lambda(x)}{\pi(x)} \right| dx \\
&= \int \mathcal{V}(x) \pi(x) \left| 1 - e^{r_2^\lambda(x) - r_1^\lambda(x) - r_2(x) + r_1(x)} \frac{\int e^{-f - r_1 + r_2}}{\int e^{-f - r_1^\lambda + r_2^\lambda}} \right| dx \\
&= \int \mathcal{V}(x) \pi(x) \left| 1 - e^{r_2^\lambda(x) - r_1^\lambda(x) - r_2(x) + r_1(x) + \beta} \cdot e^{-\beta} \frac{\int e^{-f - r_1 + r_2}}{\int e^{-f - r_1^\lambda + r_2^\lambda}} \right| dx \\
&\leq \int \mathcal{V}(x) \pi(x) \left| 1 - e^{r_2^\lambda(x) - r_1^\lambda(x) - r_2(x) + r_1(x) + \beta} \right| dx \\
&\quad + \int \mathcal{V}(x) \pi(x) e^{r_2^\lambda(x) - r_1^\lambda(x) - r_2(x) + r_1(x) + \beta} \left| 1 - e^{-\beta} \frac{\int e^{-f - r_1 + r_2}}{\int e^{-f - r_1^\lambda + r_2^\lambda}} \right| dx.
\end{aligned}$$

Since

$$r_2^\lambda(x) - r_1^\lambda(x) - r_2(x) + r_1(x) + \beta \geq 0 \quad (46)$$

it follows $e^{r_2^\lambda(x) - r_1^\lambda(x) - r_2(x) + r_1(x) + \beta} \geq 1$ and

$$e^{-\beta} \frac{\int e^{-f - r_1 + r_2}}{\int e^{-f - r_1^\lambda + r_2^\lambda}} \leq 1,$$

we have

$$\begin{aligned}
\|\pi_\lambda - \pi\|_{\mathcal{V}} &\leq \int \mathcal{V}(x) \pi(x) \left(e^{r_2^\lambda(x) - r_1^\lambda(x) - r_2(x) + r_1(x) + \beta} - 1 \right) dx \\
&\quad + \int \mathcal{V}(x) \pi(x) e^{r_2^\lambda(x) - r_1^\lambda(x) - r_2(x) + r_1(x) + \beta} \left(1 - e^{-\beta} \frac{\int e^{-f - r_1 + r_2}}{\int e^{-f - r_1^\lambda + r_2^\lambda}} \right) dx
\end{aligned}$$

Now using the evaluation (45), we derive

$$\begin{aligned}
\|\pi_\lambda - \pi\|_{\mathcal{V}} &\leq \int \mathcal{V}(x) \pi(x) \left(e^{\frac{\lambda(G_1^2 + G_2^2)}{2}} - 1 \right) dx \\
&\quad + \int \mathcal{V}(x) \pi(x) e^{\frac{\lambda(G_1^2 + G_2^2)}{2}} \left(1 - e^{-\beta} \frac{\int e^{-f - r_1 + r_2}}{\int e^{-f - r_1^\lambda + r_2^\lambda}} \right) dx
\end{aligned}$$

It also follows from (45) that

$$\frac{\int e^{-f - r_1 + r_2}}{\int e^{-f - r_1^\lambda + r_2^\lambda}} \geq e^{-\frac{\lambda G_1^2}{2}}.$$

Therefore

$$\|\pi_\lambda - \pi\|_{\mathcal{V}} \leq 2 \left(e^{\frac{\lambda(G_1^2 + G_2^2)}{2}} - 1 \right) \int \mathcal{V}(x) \pi(x) dx = O(\lambda).$$

It then follows from [Renaud et al., 2025a, Lemma 18] that (by using $\mathcal{V} = 1 + \|\cdot\|^q$)

$$W_q(\pi_\lambda, \pi) = O(\lambda^{1/q}).$$

Case 2: Assumption 4(ii):

It is a standard result that

$$r_2(x) - r_2^\lambda(x) \leq \frac{\lambda}{2} \|\nabla r_2(x)\|^2, \quad \forall x \in \mathbb{R}^d.$$

Indeed, a short proof is as follows

$$\begin{aligned} r_2(x) - r_2^\lambda(x) &= r_2(x) - \inf_y \left\{ r_2(y) + \frac{1}{2\lambda} \|x - y\|^2 \right\} \\ &= \sup_y \left\{ r_2(x) - r_2(y) - \frac{1}{2\lambda} \|x - y\|^2 \right\} \\ &\leq \sup_y \left\{ \langle \nabla r_2(x), x - y \rangle - \frac{1}{2\lambda} \|x - y\|^2 \right\} \\ &= \sup_y \left\{ -\frac{1}{2\lambda} \|y - x + \lambda \nabla r_2(x)\|^2 + \frac{\lambda}{2} \|\nabla r_2(x)\|^2 \right\} \\ &\leq \frac{\lambda}{2} \|\nabla r_2(x)\|^2. \end{aligned}$$

Under Assumption 4(ii):

$$\|\nabla r_2(x)\|^2 \leq 2(\|\nabla r_2(0)\|^2 + M^2 \|x\|^{2\kappa}).$$

Therefore

$$r_2(x) - r_2^\lambda(x) \leq \lambda(\|\nabla r_2(0)\|^2 + M^2 \|x\|^{2\kappa})$$

and

$$|r_1(x) - r_2(x) - r_1^\lambda(x) + r_2^\lambda(x)| \leq \frac{\lambda G_1^2}{2} + \lambda \|\nabla r_2(0)\|^2 + \lambda M^2 \|x\|^{2\kappa}.$$

By applying

$$|e^t - 1| \leq |t|e^{|t|}, \quad \forall t \in \mathbb{R},$$

we have

$$\begin{aligned} \|\pi_\lambda - \pi\|_{\mathcal{V}_q} &\leq \int \mathcal{V}_q(x) \pi(x) \left| 1 - e^{r_2^\lambda(x) - r_1^\lambda(x) - r_2(x) + r_1(x)} \frac{\int e^{-f - r_1 + r_2}}{\int e^{-f - r_1^\lambda + r_2^\lambda}} \right| dx \\ &\leq \int \mathcal{V}_q(x) \pi(x) \left| 1 - e^{r_2^\lambda(x) - r_1^\lambda(x) - r_2(x) + r_1(x)} \right| dx \\ &\quad + \int \mathcal{V}_q(x) \pi(x) e^{r_2^\lambda(x) - r_1^\lambda(x) - r_2(x) + r_1(x)} dx \left| 1 - \frac{\int e^{-f - r_1 + r_2}}{\int e^{-f - r_1^\lambda + r_2^\lambda}} \right| \\ &\leq \int \mathcal{V}_q(x) \pi(x) |r_2^\lambda(x) - r_1^\lambda(x) - r_2(x) + r_1(x)| e^{|r_2^\lambda(x) - r_1^\lambda(x) - r_2(x) + r_1(x)|} dx \\ &\quad + e^{\lambda G_1^2/2} \pi(\mathcal{V}_q) \left| 1 - \frac{\int e^{-f - r_1 + r_2}}{\int e^{-f - r_1^\lambda + r_2^\lambda}} \right| \\ &\leq \underbrace{\int \mathcal{V}_q(x) \pi(x) \left(\frac{\lambda G_1^2}{2} + \lambda \|\nabla r_2(0)\|^2 + \lambda M^2 \|x\|^{2\kappa} \right) e^{\frac{\lambda G_1^2}{2} + \lambda \|\nabla r_2(0)\|^2 + \lambda M^2 \|x\|^{2\kappa}} dx}_I \\ &\quad + \underbrace{e^{\lambda G_1^2/2} \pi(\mathcal{V}_q) \left| 1 - \frac{\int e^{-f - r_1 + r_2}}{\int e^{-f - r_1^\lambda + r_2^\lambda}} \right|}_II. \end{aligned}$$

Since π has sub-Gaussian tails (Appendix A),

$$\int \mathcal{V}_q(x) \|x\|^{2\kappa} e^{\lambda M^2 \|x\|^{2\kappa}} \pi(x) < +\infty \quad (47)$$

for all $\kappa \in (0, 1)$. To see this, recall $\pi \propto e^{-V}$ and there exist $a, b > 0$:

$$V(x) \geq a\|x\|^2 - b.$$

Let $\bar{a} = a/(\lambda M^2 \kappa)$. By Young's inequality

$$\|x\|^{2\kappa} \leq \frac{\kappa \bar{a}}{2} \|x\|^2 + \left(\frac{2}{\bar{a}}\right)^{\frac{\kappa}{1-\kappa}} (1-\kappa).$$

Therefore,

$$V(x) - \lambda M^2 \|x\|^{2\kappa} \geq \frac{a}{2} \|x\|^2 - c$$

for some c . So $e^{-V(x) + \lambda M^2 \|x\|^{2\kappa}}$ also has sub-Gaussian tails, which guarantees the finiteness of (47). As a result, $I = O(\lambda)$.

Now that

$$\int e^{-\lambda(\|\nabla r_2(0)\|^2 + M^2 \|x\|^{2\kappa})} \pi(x) dx \leq \frac{\int e^{-f(x) - r_1^\lambda(x) - r_2^\lambda(x)} dx}{\int e^{-f(x) - r_1(x) + r_2(x)} dx} \leq e^{\lambda G_1^2/2}.$$

Therefore,

$$\begin{aligned} \left| 1 - \frac{\int e^{-f - r_1 + r_2}}{\int e^{-f - r_1^\lambda + r_2^\lambda}} \right| &\leq \left| 1 - e^{-\lambda G_1^2/2} \right| + \left| 1 - \frac{e^{\lambda \|\nabla r_2(0)\|^2}}{\int e^{-\lambda M^2 \|x\|^{2\kappa}} \pi(x) dx} \right| \\ &\leq \lambda \frac{G_1^2}{2} e^{\lambda G_1^2/2} + \frac{|1 - e^{\lambda \|\nabla r_2(0)\|^2}| + |1 - \int e^{-\lambda M^2 \|x\|^{2\kappa}} \pi(x) dx|}{\int e^{-\lambda M^2 \|x\|^{2\kappa}} \pi(x) dx} \\ &\leq \lambda \frac{G_1^2}{2} e^{\lambda G_1^2/2} + \frac{\lambda \|\nabla r_2(0)\|^2 e^{\lambda \|\nabla r_2(0)\|^2} + \int |1 - e^{-\lambda M^2 \|x\|^{2\kappa}}| \pi(x) dx}{\int e^{-\lambda M^2 \|x\|^{2\kappa}} \pi(x) dx} \\ &\leq \lambda \frac{G_1^2}{2} e^{\lambda G_1^2/2} + \frac{\lambda \|\nabla r_2(0)\|^2 e^{\lambda \|\nabla r_2(0)\|^2} + \lambda M^2 \int \|x\|^{2\kappa} e^{\lambda M^2 \|x\|^{2\kappa}} \pi(x) dx}{\int e^{-\lambda M^2 \|x\|^{2\kappa}} \pi(x) dx} \\ &= O(\lambda) \end{aligned}$$

thanks to π having sub-Gaussian tails.

I.8 Analysis of DC-LA-S

We recall DC-LA-S

$$\begin{aligned} Y_{k+1} &= X_k - \gamma \nabla f(X_k) + \gamma \nabla r_2(X_k) + \sqrt{2\gamma} Z_{k+1} \\ X_{k+1} &= \text{Prox}_{\gamma r_1^\lambda}(Y_{k+1}). \end{aligned}$$

Similar to Section 4.1, Y_{k+1} is formulated as

$$Y_{k+1} = Y_k - \gamma b_\lambda^\gamma(Y_k) + \sqrt{2\gamma} Z_{k+1} \quad (48)$$

where the drift is

$$b_\lambda^\gamma(y) := \nabla r_1^\lambda(\text{Prox}_{\gamma r_1^\lambda}(y)) + \nabla f(\text{Prox}_{\gamma r_1^\lambda}(y)) - \nabla r_2(\text{Prox}_{\gamma r_1^\lambda}(y)). \quad (49)$$

b_λ^γ is $(L_f + \frac{1}{\lambda} + L_{r_2})$ -smooth. Similar to the evaluations in I.3, for $\gamma \leq \gamma_0$, we have

$$\langle b_\lambda^\gamma(x) - b_\lambda^\gamma(y), x - y \rangle \geq \mu \|x - y\|^2 - 2G_1(2 + L_f\gamma_0 + L_{r_2})\|x - y\|$$

for $\|x - y\| \geq R_0$. Therefore, b_λ^γ is $(\frac{\mu}{2}, R)$ -distant dissipative where

$$R := \max \left\{ R_0, \frac{4G_1(2 + L_f\gamma_0 + L_{r_2})}{\mu} \right\}.$$

We next define another drift

$$\bar{b}_\lambda^\gamma(y) = \nabla r_1^\lambda(\text{Prox}_{\gamma r_1^\lambda}(y)) + \nabla f(y) - \nabla r_2(y), \quad (50)$$

and the corresponding general ULA:

$$\bar{Y}_{k+1} = \bar{Y}_k - \gamma \bar{b}_\lambda^\gamma(\bar{Y}_k) + \sqrt{2\gamma} \bar{Z}_{k+1}. \quad (51)$$

We also denote

$$\pi_{\lambda, \gamma}(x) \propto \exp(-f(x) - (r_1^\lambda)^\gamma(x) + r_2(x)),$$

then it follows that $-\nabla \log \pi_{\lambda, \gamma} = \bar{b}_\lambda^\gamma$.

Similarly, we can show that: for all $\gamma > 0$, \bar{b}_λ^γ is $(\frac{1}{\lambda} + L_f + L_{r_2})$ -smooth and is $(\frac{\mu}{2}, \bar{R})$ -distant dissipative where

$$\bar{R} = \max \left\{ R_0, \frac{8G_1}{\mu} \right\}.$$

Let Q, \bar{Q} be transition kernels of $\{Y_k\}_k$ and $\{\bar{Y}_k\}_k$, respectively. According to Lemma 12, Q, \bar{Q} admit invariant distributions called $p_{\lambda, \gamma}, \bar{p}_{\lambda, \gamma} \in \mathcal{P}_1(\mathbb{R}^d)$. Furthermore, if $q \geq 2$, Lemma 12 guaranties $p_{\lambda, \gamma}, \bar{p}_{\lambda, \gamma} \in \mathcal{P}_{2q}(\mathbb{R}^d)$.

Similar to the arguments in Section I.5, there exist $C_{1,q}(\lambda), C_{2,q}(\lambda), C_{3,q}(\lambda) > 0$ and $\rho_{q,\lambda} \in (0, 1)$ such that

$$W_q(p_{Y_{k+1}}, \pi_{\lambda, \gamma}) \leq C_{1,q}(\lambda) \rho_{q,\lambda}^{k\gamma/q} + C_{2,q}(\lambda) (L_f + L_{r_2})^{\frac{1}{q}} G_1^{\frac{1}{q}} \gamma^{\frac{1}{q}} + C_{3,q}(\lambda) \gamma^{\frac{1}{2q}}.$$

Finally, we can apply [Renaud et al., 2025a, Proposition 1] two times to get

$$\begin{aligned} W_q(\pi_{\lambda, \gamma}, \pi_\lambda) &= O(\gamma^{1/q}) \\ W_q(\pi_\lambda, \pi) &= O(\lambda^{1/q}). \end{aligned}$$

J Additional experimental results and details

J.1 Standard proximal operators

It is well-known that the proximal operators of ℓ_1 and ℓ_2 are given by

$$\begin{aligned} \text{Prox}_{\gamma \ell_1}(x) &= \text{sign}(x) \odot \max(|x| - \gamma, 0), \\ \text{Prox}_{\gamma \ell_2}(x) &= \max \left(1 - \frac{\gamma}{\|x\|_2}, 0 \right) x. \end{aligned}$$

Recently, Lou and Yan [2018] showed that the proximal operator of $\ell_1 - \ell_2$, or more generally, $\ell_1 - \epsilon \ell_2$ with $\epsilon > 0$, is given in closed form as

$$\text{Prox}_{\gamma(\ell_1 - \epsilon \ell_2)}(x) \ni \begin{cases} 0, & \text{if } \|x\|_\infty \leq (1 - \epsilon)\gamma, \\ \left(1 + \frac{\epsilon\gamma}{\|\text{Prox}_{\gamma \ell_1}(x)\|_2} \right) \text{Prox}_{\gamma \ell_1}(x), & \text{if } \|x\|_\infty > \gamma, \\ \text{sign}(x_{i^*})(\|x\|_\infty + (\epsilon - 1)\gamma)e_{i^*}, & \text{if } (1 - \epsilon)\gamma < \|x\|_\infty \leq \gamma, i^* = \arg \max_i |x_i|. \end{cases}$$

Note that, in the above formulation, whenever $\text{prox}_{\gamma(\ell_1 - \epsilon\ell_2)}(x)$ is set-valued, we use an arbitrary but fixed single-valued selection (any element of the proximal set), which suffices for implementation.

J.2 $\ell_1 - \ell_2$ prior

Histograms of samples from multiple chains With the same setups as in Subsection 5.1, we do the experiments with other covariance matrices, including the identity $\begin{bmatrix} 1 & 0 \\ 0 & 1 \end{bmatrix}$ and $\begin{bmatrix} 1 & -0.8 \\ -0.8 & 2 \end{bmatrix}$. Figures 5 and 6 show the histograms of DC-LA, PSGLA, Moreau ULA and ULA. Figures 7 and 8 show the binned KL divergence between the histograms of samples generated by each sampling algorithm and the binned target distribution. In these cases, DC-LA achieves the lowest binned KL divergence.

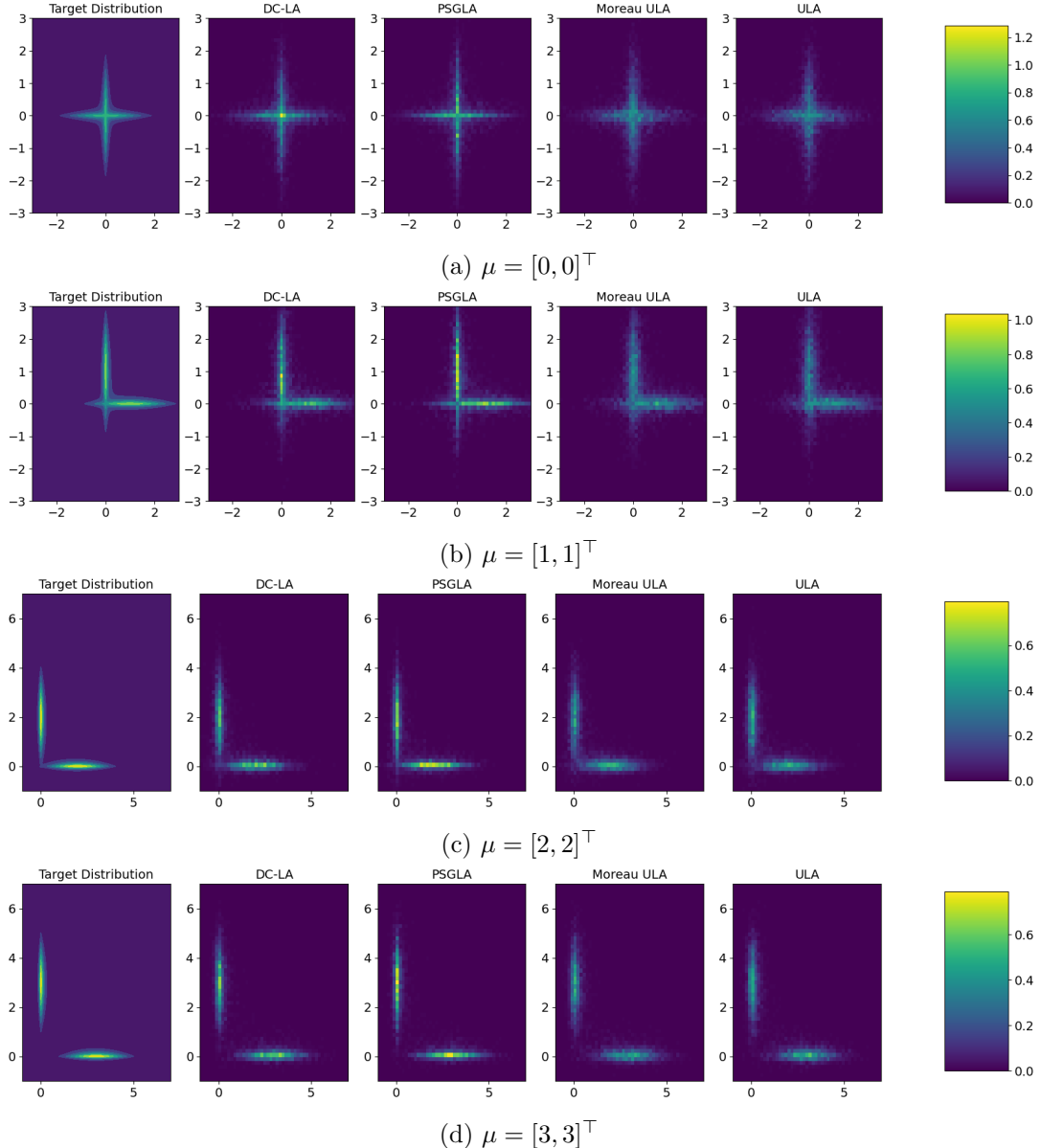


Figure 5: $\Sigma = \begin{bmatrix} 1 & 0 \\ 0 & 1 \end{bmatrix}$, multiple chains

Histograms of samples from a single chain We also report histograms based on samples obtained from a single Markov chain of length 10,000, discarding the first 500 samples as burn-in.

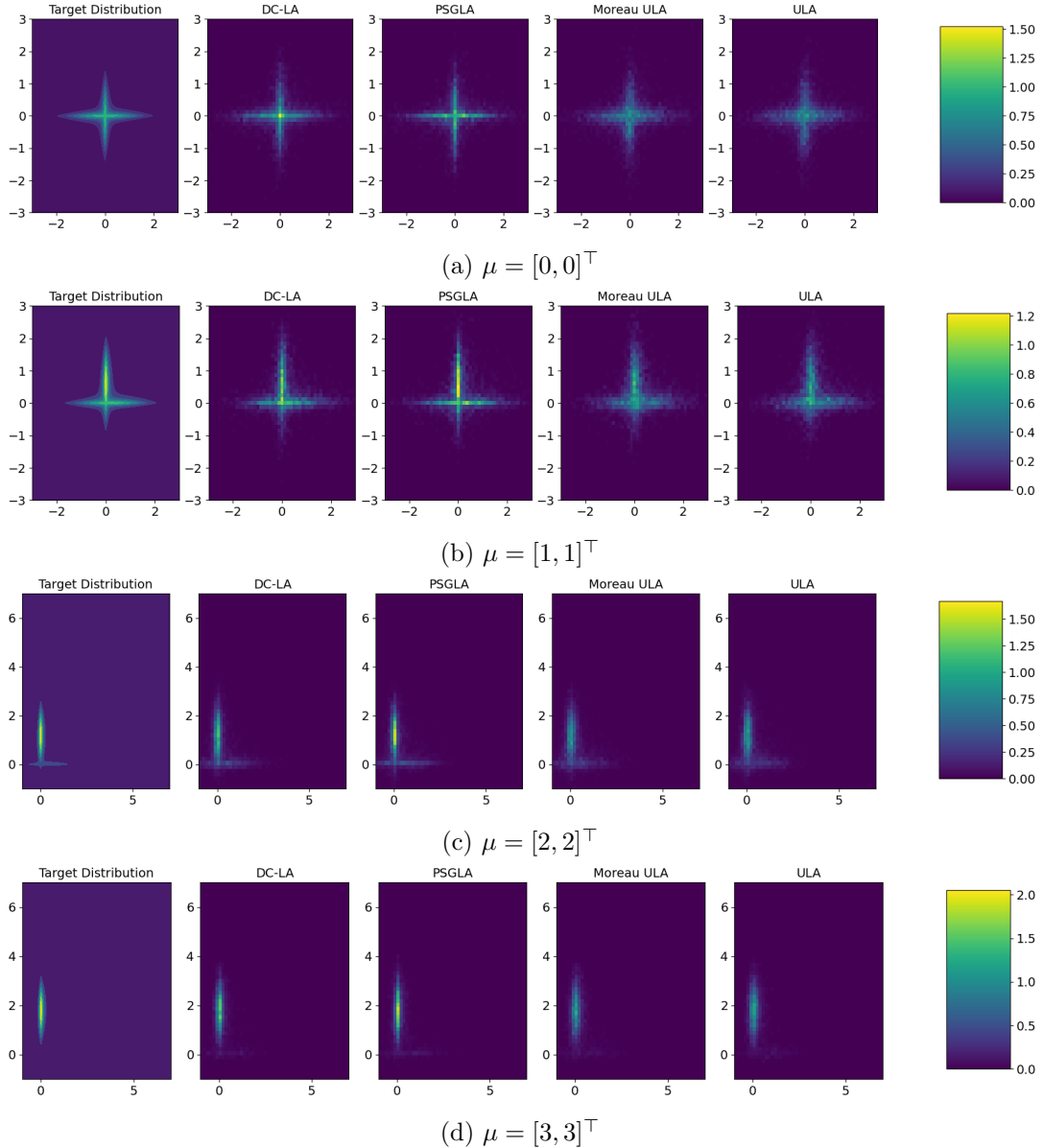


Figure 6: $\Sigma = \begin{bmatrix} 1 & -0.8 \\ -0.8 & 2 \end{bmatrix}$, mutiple chains

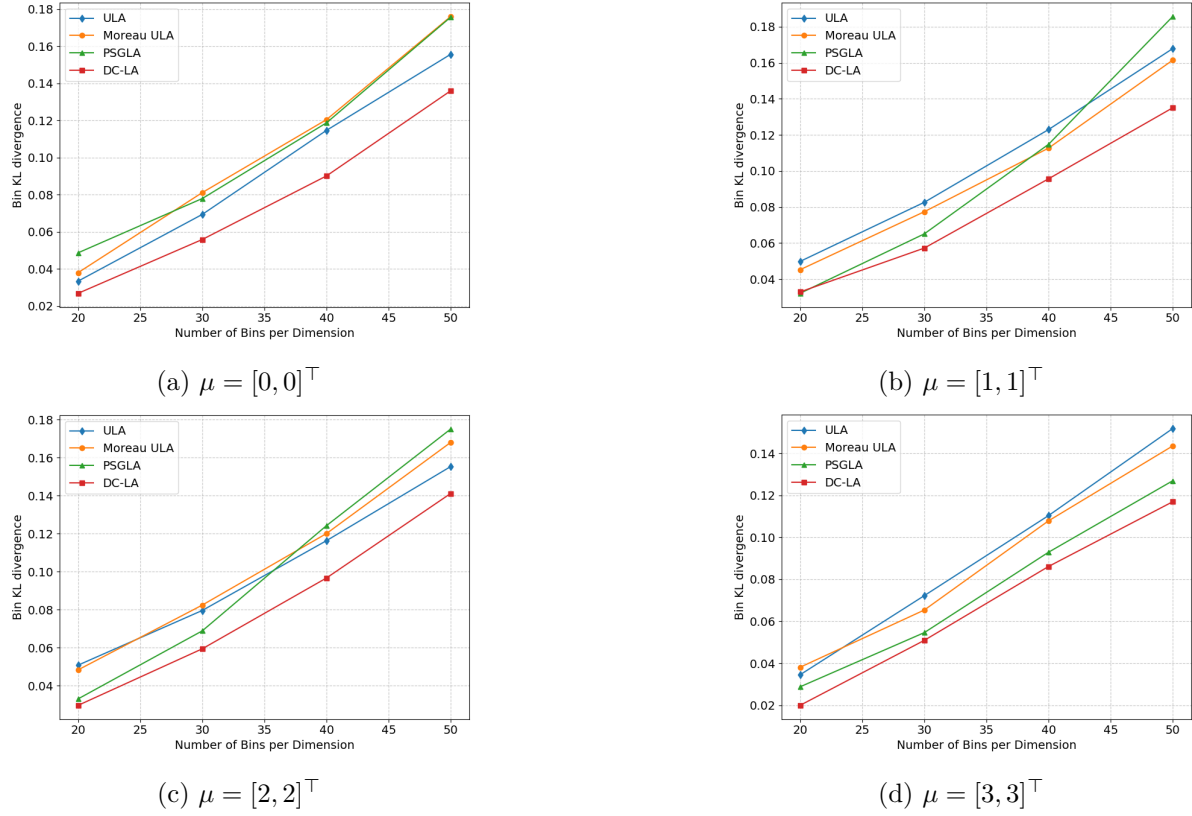


Figure 7: $\Sigma = \begin{bmatrix} 1 & 0 \\ 0 & 1 \end{bmatrix}$, mutiple chains

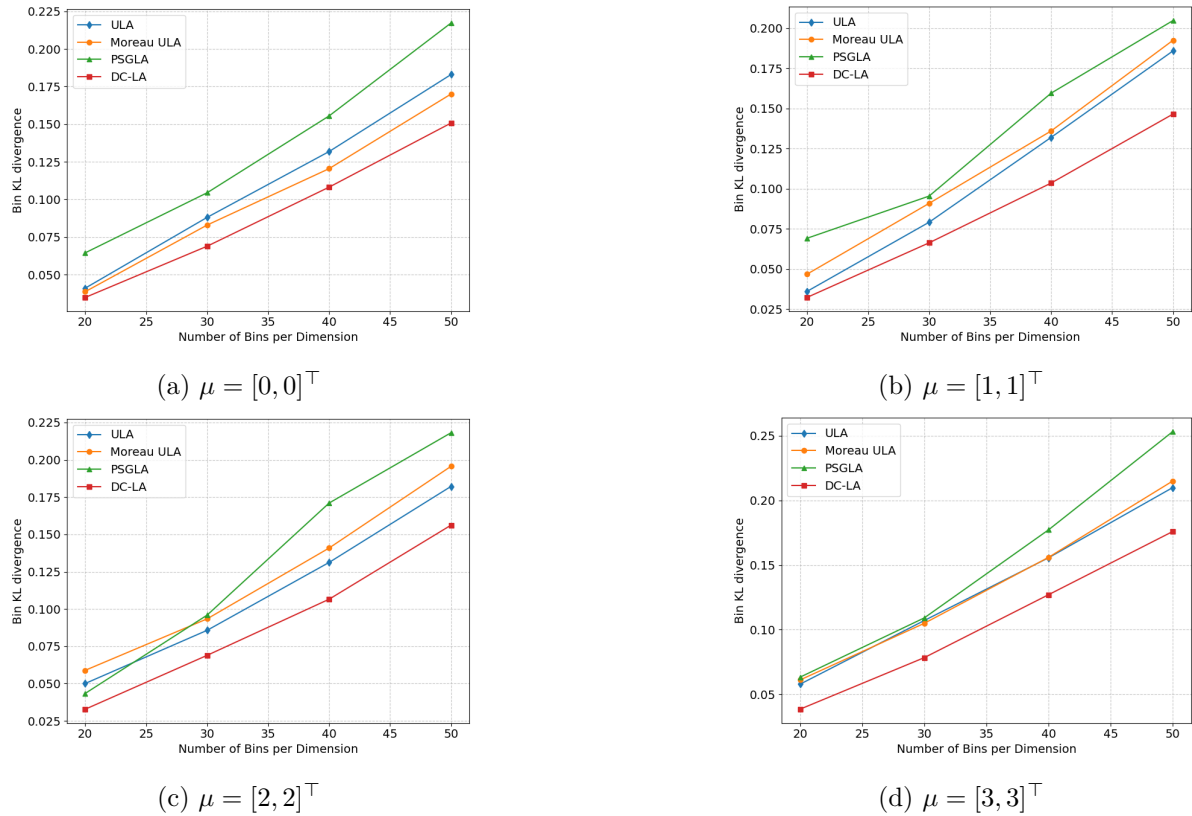


Figure 8: $\Sigma = \begin{bmatrix} 1 & -0.8 \\ -0.8 & 2 \end{bmatrix}$, mutiple chains

Although our theoretical results apply to multiple chains using the final sample from each, it is common practice to run a single long chain and obtain samples directly from it. Figures 9 and 10 show the histograms of single chains of four samplers. As expected, the fidelity is lower than when running multiple chains. Still, DC-LA achieves a good compromise between ULA/Moreau ULA and PSGLA, although all algorithms struggle to efficiently explore every mode.

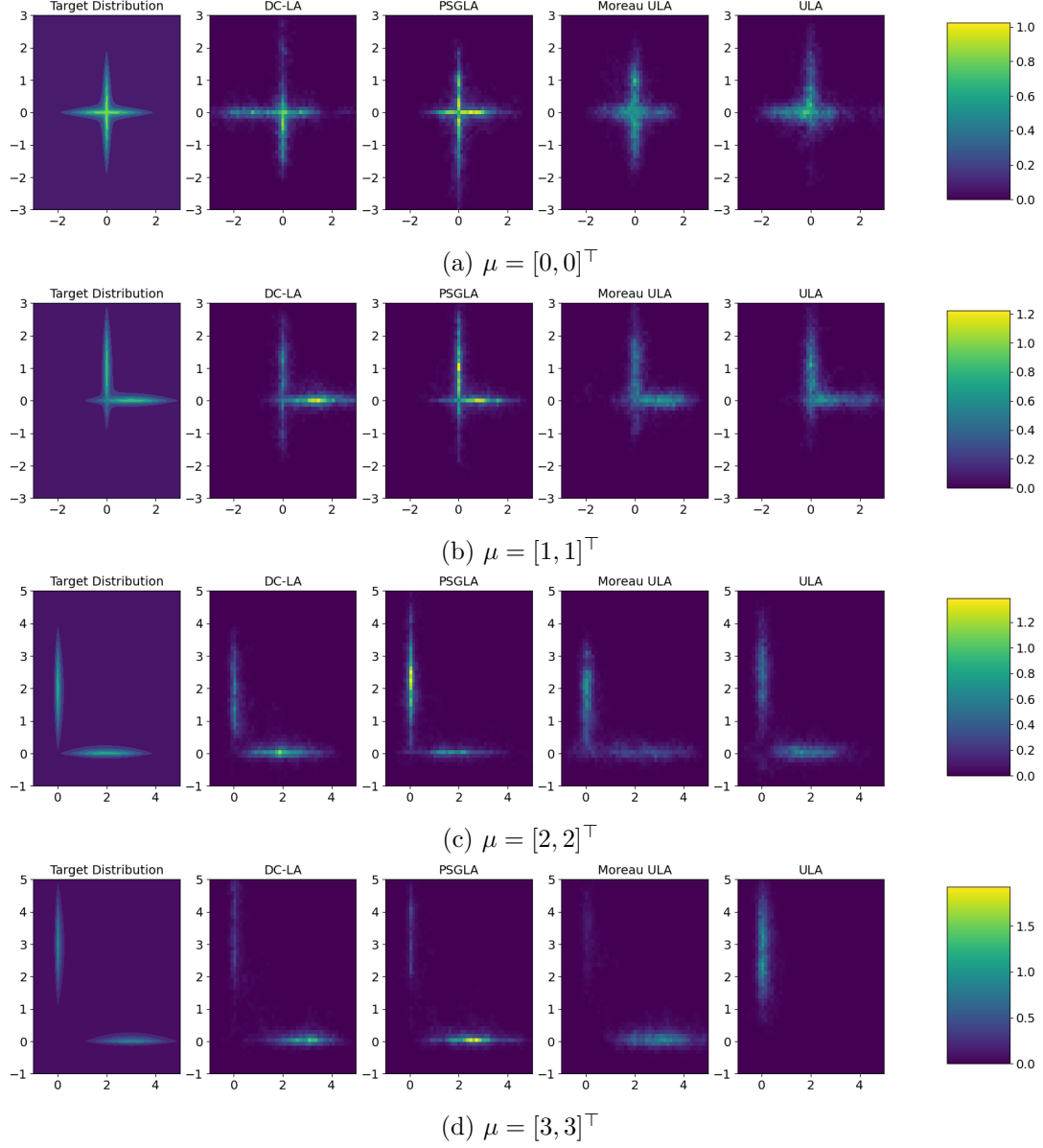


Figure 9: $\Sigma = \begin{bmatrix} 1 & 0 \\ 0 & 1 \end{bmatrix}$, single chain

Ablation experiment on (λ, γ) We study the sensitivity of the performance of DC-LA with respect to the smoothing parameter λ and the step size γ . To this end, we sweep $\lambda \in \{10^{-4}, 3 \times 10^{-4}, 10^{-3}, 3 \times 10^{-3}, 10^{-2}, 3 \times 10^{-2}\}$ and $\gamma \in \{10^{-4}, 3 \times 10^{-4}, 10^{-3}, 3 \times 10^{-3}, 10^{-2}\}$. For each grid point (λ, γ) , we run 3000 DC-LA chains of length 1000 and keep the last sample of each chain. Figure 11 shows the performance of DC-LA when (λ, γ) varies. We observe a broad region of stable performance for intermediate values of both parameters. The consistency across all 12 subplots suggests that while the absolute error scale changes (the color bar ranges), the optimal "sweet spot" for hyperparameters remains relatively stable, indicating that DC-LA is robust and does not require drastic retuning when the underlying data distribution (mean

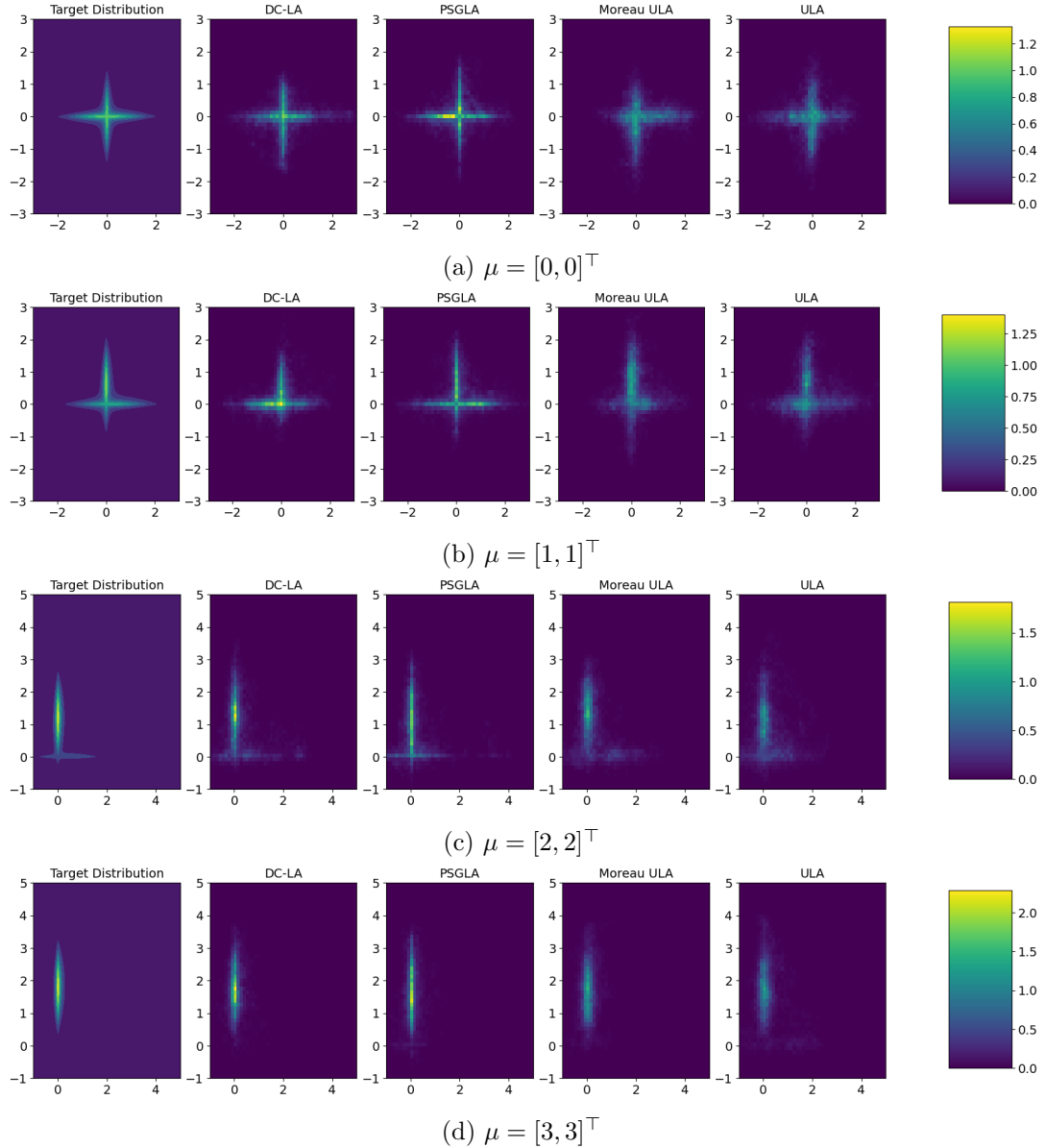


Figure 10: $\Sigma = \begin{bmatrix} 1 & -0.8 \\ -0.8 & 2 \end{bmatrix}$, single chain

or correlation) shifts. In this experiment, we see that setting γ on the order of λ (but a factor smaller) provides a favorable balance, yielding stable behavior while still allowing the chain to mix quickly.

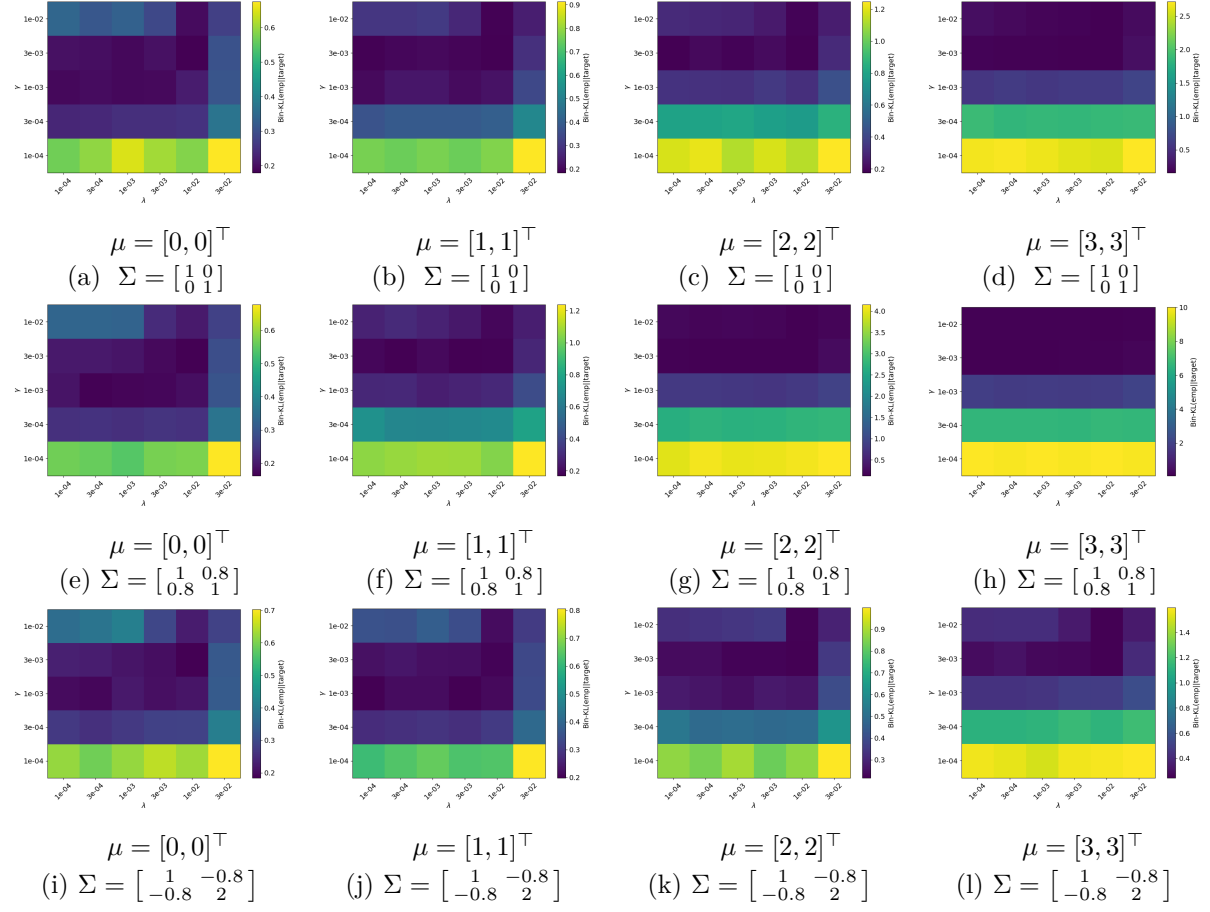
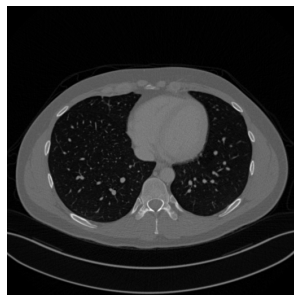


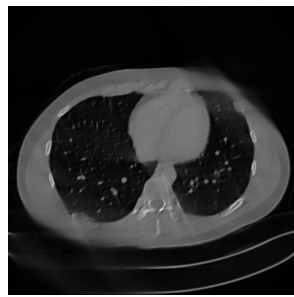
Figure 11: Ablation experiment analyzing the sensitivity of DC-LA performance to the hyperparameters (λ, γ) .

J.3 Computed Tomography with DCINNs prior

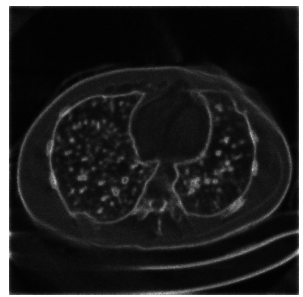
We show in Figures 12, 13, 14, and 15 some other results with the same settings as in Section 5.2. Here, the caption of each figure indicates the corresponding CT scan code name in the original dataset Moen et al. [2021].



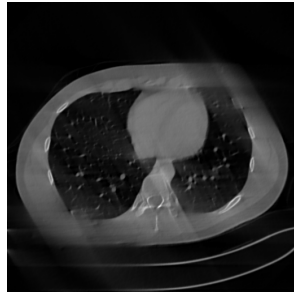
(a) Ground truth



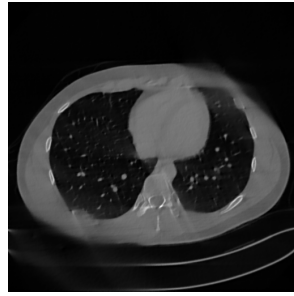
(b) Estimated mean by DC-LA (SSIM: 0.8551, PSNR: 26.9296)



(c) Estimated pixel-wise variance by DC-LA



(d) Estimated MAP by PSM at iteration 2000 (SSIM: 0.7709, PSNR: 24.7982)

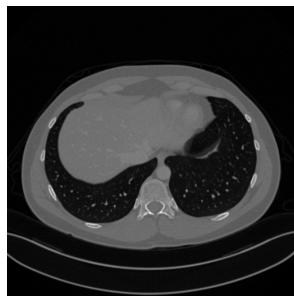


(e) Estimated MAP by PSM at iteration 10000 (SSIM: 0.8548, PSNR: 26.9454)

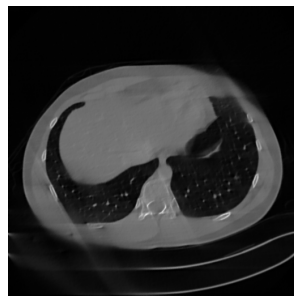


(f) Estimated MAP by PSM at iteration 20000 (SSIM: 0.8547, PSNR: 27.0340)

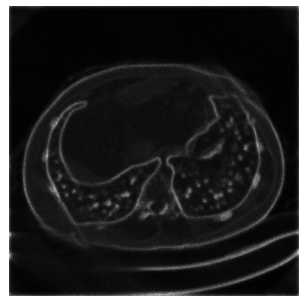
Figure 12: Scan: L333_FD_1_1.CT.0002.0010.2015.12.22.20.18.21.515343.358517203



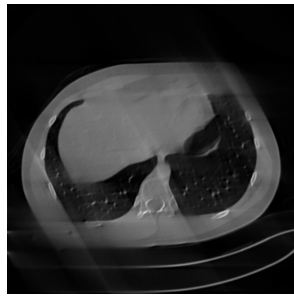
(a) Ground truth



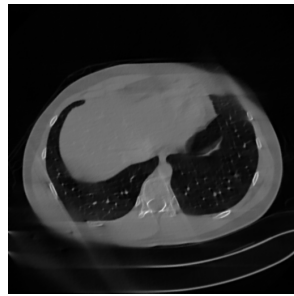
(b) Estimated mean by DC-LA (SSIM: 0.8702, PSNR: 27.4151)



(c) Estimated pixel-wise variance by DC-LA



(d) Estimated MAP by PSM at iteration 2000 (SSIM: 0.7972, PSNR: 25.1140)

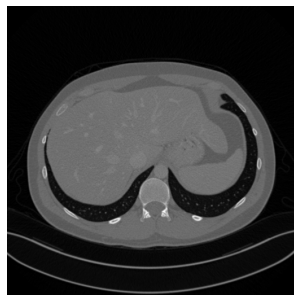


(e) Estimated MAP by PSM at iteration 10000 (SSIM: 0.8702, PSNR: 27.4418)

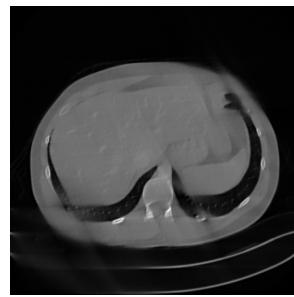


(f) Estimated MAP by PSM at iteration 20000 (SSIM: 0.8712, PSNR: 27.7555)

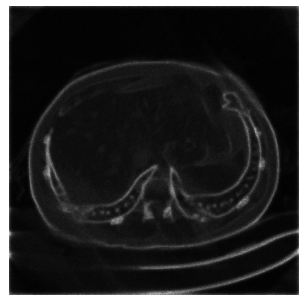
Figure 13: Scan: L333_FD_1_1.CT.0002.0050.2015.12.22.20.18.21.515343.358518163



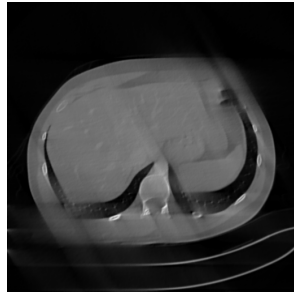
(a) Ground truth



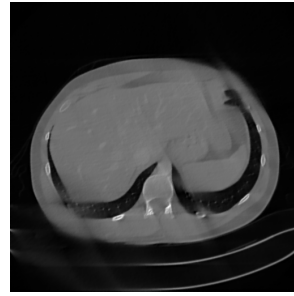
(b) Estimated mean by DC-LA (SSIM: 0.8666 , PSNR: 26.9199)



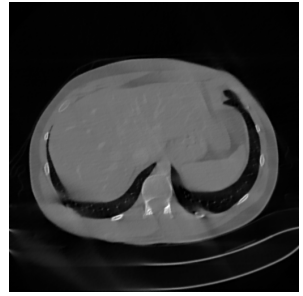
(c) Estimated pixel-wise variance by DC-LA



(d) Estimated MAP by PSM at iteration 2000 (SSIM: 0.7997, PSNR: 25.1084)

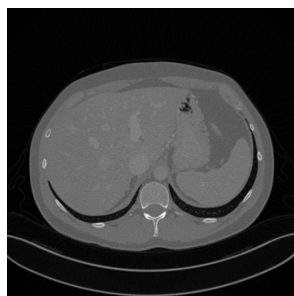


(e) Estimated MAP by PSM at iteration 10000 (SSIM: 0.8664, PSNR: 26.9521)

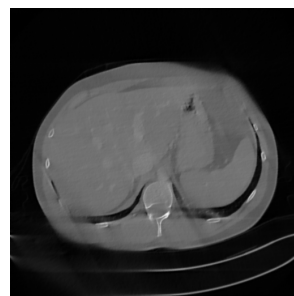


(f) Estimated MAP by PSM at iteration 20000 (SSIM: 0.8641, PSNR: 27.2395)

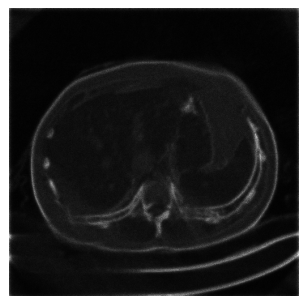
Figure 14: Scan: L333_FD_1_1.CT.0002.0080.2015.12.22.20.18.21.515343.358518883



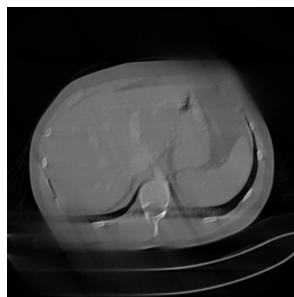
(a) Ground truth



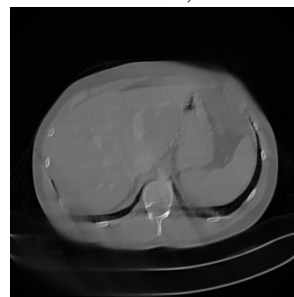
(b) Estimated mean by DC-LA (SSIM: 0.8680, PSNR: 27.6531)



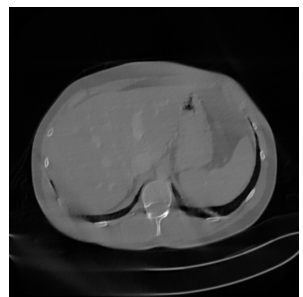
(c) Estimated pixel-wise variance by DC-LA



(d) Estimated MAP by PSM at iteration 2000 (SSIM: 0.8092, PSNR: 26.1647)



(e) Estimated MAP by PSM at iteration 10000 (SSIM: 0.8672, PSNR: 27.6856)



(f) Estimated MAP by PSM at iteration 20000 (SSIM: 0.8633, PSNR: 27.4784)

Figure 15: Scan: L333_FD_1_1.CT.0002.0100.2015.12.22.20.18.21.515343.358519363